

博士論文

Studies on severe manifestations in experimental rodent malaria
(ネズミマラリアにおける重症症状に関する研究)

山越 祥子

Contents

Contents	2
Abbreviations	4
General introduction	6

Chapter 1

Clinical features in *Plasmodium berghei*-infected C57BL/6 and BALB/c mice.

Abstract	10
1.1 Introduction	11
1.2 Materials and methods	14
1.3 Results	18
1.4 Discussion	22

Chapter 2

Cerebral edema in *Plasmodium berghei*-infected C57BL/6 mice.

Abstract	25
2.1 Introduction	26
2.2 Materials and methods	29
2.3 Results	32
2.4 Discussion	34

Chapter 3

Pulmonary edema in *Plasmodium berghei*-infected C57BL/6 mice.

Abstract	38
3.1 Introduction	39
3.2 Materials and methods	41
3.3 Results	43
3.4 Discussion	44

Chapter 4

Stillbirth with dynamic structural change of placenta occurred in
Plasmodium berghei-infected pregnant C57BL/6 mice.

Abstract	47
4.1 Introduction	48
4.2 Materials and methods	52
4.3 Results	56
4.4 Discussion	59

Conclusion	62
Acknowledgements	66
References	67
Tables	76
Figure legends	79
Figures	88
Abstract (in Japanese)	122

Abbreviations

ALB	albumin
ALT	alanine aminotransferase
AST	aspartate aminotransferase
AMY	amylase
BBB	blood-brain barrier
BCS	Blantyre Coma Scale
BUN	blood urea nitrogen
Ca	calcium
Cl	chlore
CRE	creatinine
CSF	cerebrospinal fluid
DAB	3,3'-diaminobenzidine thtrahydrochloride
dpi	days post infection
Fe	iron
GCS	Glasgow Coma Score
GLU	glucose
G1	gestation day one
γ -GT	γ -glutamyltransferase
HBSS	Hanks' Balanced Salt Solution
HDL-C	high-density lipoprotein
HE	hemotoxylin eosin
IgG	Immunoglobulin G
IUGR	fetal intrauterine growth restriction
IP	inorganic phosphorus
i.p.	intraperitoneal
i.v.	intravenous
K	kalium
LDH	lactase dehydrogenase
Na	natrium
PBS	phosphate-buffered saline

pRBCs	parasitized red blood cells
RMCBS	rapid murine coma and behavior scale
RBCs	red blood cells
T-BIL	total bilirubin
T-CHO	total cholesterol
TG	triglyceride
TP	total protein
WBCs	white blood cells

General introduction

Plasmodium parasites

Plasmodium is a genus of parasitic protozoa. Infection with *Plasmodium* parasites is known as malaria. The parasite always has two hosts in its life cycle: a mosquito vector and a vertebrate host. Four species infect humans. Other species infect other animals, including birds, reptiles and rodents.

Plasmodium parasites and their vertebrate hosts

Plasmodium vivax, *P. ovale*, *P. malariae*, and *P. falciparum* are the four species infecting humans and cause malaria. Malaria is one of the major tropical diseases. This parasitic infection results in 200 to 300 million clinical cases and 1 to 2 million deaths annually, mostly children under 5 and pregnant women in sub Saharan Africa (Penet et al., 2007). *P. falciparum* infection causes the most virulent and deadly infections (Chang & Stevenson, 2004). Among monkeys, *P. cynomolgi*, infecting *macaca fascicularis* in Java or Malayan and *P. knowlesi*, infecting *macaca irus* in Asia are famous (Collins et al., 1992). Recently, Some human cases of *P. knowlesi* infection were reported (Singh et al., 2004). Among reptiles, there are a lot of *Plasmodium* parasites can infect to lizard like *P. sasai*, infecting to Japanese

grass lizard (*Takydromus tachydromoides*) (Telford, 1998). Additionally, there are some unique parasites like *P. mexicanum*, infecting to *Sceloporus ferrariperezi* in Mexico. The vector of *P. mexicanum* is not mosquito but sandfly (*Lutzomyia vexatrix occidentis* or *Lutzomyia stewardi*) (Vardo-Zalik & Schall, 2009). Also *Plasmodium* parasites can infect turtles and snakes were reported. Among birds, *P. cathemerium*, *P. circumflexum* and *P. elongatum* are known since early time (Salakij, Lertwatcharasarakul, Kasorndorkbua, & Salakij, 2012; Wiersch, Maier, & Kampen, 2005). Recently, *P. relictum* are reported the cause of mortality in penguins and considered a social problem in the world (Atkinson & Samuel, 2010). Also *P. gallinaceum*, infecting to *gallus gallus domesticus* is famous and used for experiment (Ceneviva & Camargo, 1979). As just describe, there are a lot of *Plasmodium* parasites cause of host malaria [Fig. 1] . However, the pathogenesis of *Plasmodium* infection is poorly understood. In this study, I focused on the one of hosts, mouse, which can be used established experimental infection.

Experimental rodent malaria

In 1948, the first rodent *Plasmodium* parasite was discovered in thicket rats of the Katanga region of the then Belgian Congo. This parasite, *P. berghei*, which proved to be infective to laboratory mice, rats, and hamsters, has been widely exploited for the past 50 years for research on malaria immunology and chemotherapy research. Since 1948, other murine *Plasmodium* parasites, *P. chabaudi*, *P. vinckei* and *P. yoelli* were discovered

(Mackinnon, Gaffney, & Read, 2002). The *Plasmodium* life cycle includes firstly a non-pathogenic symptomless hepatocyte stage followed by a pathogenic red blood cell stage. Transmission via the bite of an infected female *Anopheles* species mosquito induces the hepatocyte stage; sporozoites invade hepatocytes, replicate, and produce merozoites, and these later initiate the red blood cell stage with invasion of red blood cells. During the red blood cell stage, clinical malaria may develop (Penet et al., 2007). In experimental rodent *Plasmodium* infection, infection with pRBCs is a technique often used to skip the non-pathogenic symptomless hepatocyte stage of the parasite cycle. They directly undergo the red blood cell stage, which is a symptomatic stage. In this study, I tried to clarify the part of mechanism of experimental rodent malaria pathogenesis by *P. berghei*-infection to two kinds of inbred mice, C57BL/6 and BALB/c.

Chapter 1

Clinical features in *Plasmodium berghei* infected C57BL/6 and BALB/c mice.

Abstract

Plasmodium is a genus of parasitic protozoa. Infection with *Plasmodium* parasites is known as malaria. However, the pathogenesis of *Plasmodium* infection is poorly understood. In this study, I focused on the one of hosts, mouse, which can be used established experimental infection. I designed objective of this study to reveal what kind of manifestations occurred in *P. berghei*-infected C57BL/6 and BALB/c. 1×10^6 *P. berghei* ANKA were inoculated to C57BL/6 and BALB/c. I performed the blood examination, consciousness and movement test, and autopsy. The parasitemia occurred in both C57BL/6 and BALB/c. Its growth rate was not different among strain. Anemia, splenomegaly, liver and gallbladder injury occurred in both strains. On the other hand, consciousness and movement disturbance, respiration failure and abnormal bleeding occurred only in *P. berghei*-infected C57BL/6. These results indicated that *P. berghei*-infected C57BL/6 had several severe manifestations that weren't occurred in BALB/c even though rate of infection was same.

1.1 Introduction

For examinations of clinical features of experimental rodent malaria, I referred to the clinical features of human malaria and its diagnostic approach.

The clinical features in human malaria

The classic clinical features of human malaria are parasitemia, anemia, splenomegaly and fever accompanied by other symptoms such as headache, malaise, nausea, muscular pains and mild diarrhea (Pasvol, 2005; White et al., 2013). Initially, parasitemia is a first clinical finding by microscopic examination. Subsequently, typical symptoms of malaria such as fever, anemia, and splenomegaly appear accompanied with development of parasitemia. The majority of cases present as a relatively mild, non-specific febrile illness which resolves rapidly if treated appropriately, however, some cases often leads severe, life threatening, malaria which has a complex pathogenesis within a short time. The most lethal cases are occurred by *P. falciparum* infection. In WHO, the severe manifestations from infection *P. falciparum* are defined as severe malaria clinical features of severe malaria is cerebral malaria (impaired consciousness, including unrousable coma),

prostration, multiple convulsions (more than two episodes within 24h), deep breathing and respiratory distress (acidotic breathing), acute pulmonary edema and acute respiratory distress syndrome, circulatory collapse or shock, acute kidney injury, hypoglycaemia, metabolic acidosis, severe anemia, hemoglobinuria, hyperlactatemia, renal impairment, clinical jaundice and abnormal bleeding. The manifestations of severe malaria depend of age. Severe anemia and hypoglycaemia are more common in children, whereas acute pulmonary edema, acute kidney injury, and jaundice are more common in adults. Cerebral malaria and acidosis occur in all age groups [Fig. 2] .

The diagnosis of human malaria

The parasitological direct detection is most important in the diagnosis for human malaria because it can mimic many other diseases that are also common in malaria-endemic countries. Microscopy is the gold standard and preferred option for diagnosing malaria. In nearly all cases, examination of thick and thin blood smears will reveal *Plasmodium* parasite. Thick smears are more sensitive than thin smears for detecting low-density parasitemia. Parasitemia > 2% is associated with high risk in any epidemiological context. Anemia are diagnosed by the amount of hemoglobin of hematocrit level. The cases of concentration of hemoglobin < 5 g/dL in, hematocrit level < 15% in children, hemoglobin < 7 g/dL in, hematocrit level < 20% in adults sre diagnosed as severe aneamia. Cerebral malaria is diagnosed clinically

using a GCS for adults, or a BCS for children (Carroll et al., 2010; Snow, Guerra, Noor, Myint, & Hay, 2005). Acute pulmonary edema is diagnosed by X-ray examination. Circulatory collapse or shock are diagnosed by examination of blood pressure, < 80mm Hg in adults and <50 mm Hg in children. Acute kidney injury, hypoglycaemia, hyperlactatemia and renal impairment are diagnosed by biochemical examination of blood (hypoglycaemia < 40 mg/dl, hyperlactatemia, lactate > 5 mmol/l, renal impairment, serum creatinine > 265 μ mol/L). Metabolic acidosis is diagnosed by examination of plasma bicarbonate < 15 mmol/L (Pasvol, 2005). Based on these clinical features in human, I performed the blood examinations, conscious and behavior test and the autopsy in experiment rodent malaria.

1.2 Materials and methods

Animals and parasites

All animal procedures in this study were approved by the Committee for Experimental Animals at the University of Tokyo. Eight week-old C57BL/6 and BALB/c female mice were obtained from Japan Clea, Tokyo, Japan, and housed under specific pathogen-free conditions with free access to food and water. *Plasmodium berghei* ANKA was used for this study. Malaria parasites were stored as frozen stocks in liquid nitrogen. pRBCs of *P. berghei* ANKA were generated in donor mice inoculated i.p. with frozen stock of parasites.

Experimental infection

To prepare pRBCs, blood was collected from donor mice and mixed well with Citrate-phosphate-dextrose as anticoagulant. The pRBCs were washed two times with HBSS (Life Technologies, Carlsbad, CA) by centrifugation at 400 $\times g$ for 5 min. Thirteen mice of each strain were infected by i.p. injection of 10^6 pRBCs. From five of them, weight, RMBCS score and the number of breaths per minute were monitored on dpi 0, 2, 4 and 6. Also parasitemia was monitored every day. Other five mice were used for blood biochemical examination. Remaining three mice were used for assessment of hematocrit level.

Parasite detection

Blood was collected from the tail every day (n=5). To monitor parasitemia level, thin blood smears were fixed with methanol for 5 min and then stained for 25 min with 5% Giemsa stain in PBS (pH 7.4). A thousand RBCs (including pRBCs) were counted for each mouse by the microscopic examination. The pRBCs rate was expressed as percentage of pRBCs in 1000 counted RBCs.

Assessment of hematocrit level

Hematocrit levels were assessed on dpi 0, 2, 4 and 6 (n=3). A fresh sample of blood is collected from tails and introduced into capillary tubes coated with heparin. The end of tubes was sealed with putty and they were centrifuged at 13,000 g for 5 min. The straw colored supernatant is the plasma, the RBCs sink to the bottom, and the WBCs are seen as a thin buffy coat at the top of the RBCs column. By determining the percent of the total represented by the packed cells, the percent of RBCs in whole blood can be determined. Naive mice were assessed by same way as a control.

Blood biochemical examination

Whole blood of infected mice was collected from heart on dpi 6 (n=5). The blood was centrifuged at 5,000 g for 10 min and collected serum. The concentrations of TP, ALB, BUN, CRE, Na, K, Cl, Ca, IP, Fe, AST, ALT, LDH, AMY, γ -GT, T-CHO, TG, HDL-C, GLU and T-BIL in the serum of mice were measured by using biochemistry automatic analyzer (7180 Clinical Analyzer, Hitachi High-Tec.Corp. ,Tokyo, Japan).

RMCBS test

The RMCBS test was examined as described by Carroll. et al. (Carroll et al., 2010). The RMCBS consists of 10 parameters, and each parameter is scored 0 to 2, with a 0 score correlating with the lowest function and a 2 score, the highest. An animal can achieve an accumulative score of 0 to 20. During the first 90 seconds of assessment, the mouse is placed in the top left corner of an observation box (length, 31.8 cm, width, 19.8 cm, height, 10.5 cm) with a grid floor and is assessed for hygiene- related behavior, gait, body position, exploratory behavior, and balance. In the subsequent 90 seconds, the mouse is assessed for reflexes, limb strength, and self-preservation actions. An illustrative table [Table 1] is provided for more specific descriptions of the assessments. Infected mice were assessed via the RMCBS on dpi 0, 2, 4 and 6 (n=5). Attempts were made to assess the mice at the same time each day, usually the evening hours, for every experiment. Naive mice were assessed

by same way as a control. The weight of mice was also monitored in same days.

The number of breaths counting

Infected mice were fixed by a retainer and measured the number of breaths for 60 seconds by visual observation (n=5). Mice were assessed on dpi 0, 2, 4 and 6. Naive mice were assessed by same way as a control.

Autopsy

Mice were sacrificed and performed the autopsy in dpi 6 (n=5). The brains, livers, gallbladders, kidneys, spleens, lungs, adrenal glands and skins were removed from infected mice. The color alternation of organs was examined grossly and the weight of the spleens was measured.

Statistical analysis

Statistical analyses were performed by *t*-test, and *p* values less than 0.01 were considered statistically significant.

1.3 Results

Increase of pRBCs

From dpi 3, pRBC were observed in peripheral blood for the first time [Fig. 3B] , and pRBC rate was elevated over the course of infection. On dpi 6, the mean \pm SD of parasitemia of 5 mice was 36.37 ± 5.37 % in C57BL/6 and 37.14 ± 8.48 % in BALB/c [Fig. 3A] .

Decrease hematocrit level

Hematocrit level was monitored on dpi 0, 2, 4 and 6. Hematocrit levels in C57BL/6 and BALB/c were decreased with progression of infection. On dpi 6, the mean \pm SD of hematocrit level of 3 infected C57BL/6 ($32.67 \pm 2.33\%$) was significantly lower than the naive one ($47.33 \pm 1.45\%$). The mean \pm SD of hematocrit level of 3 infected BALB/c ($29.67 \pm 3.93\%$) was significantly lower than the naive one ($52.33 \pm 1.45\%$) [Fig. 4] .

Concentrations of serum components

On dpi 6, the concentrations of TP, ALB, BUN, CRE, Na, K, Cl, Ca, IP, Fe, AST, ALT, LDH, AMY, γ -GT, T-CHO, TG, HDL-C, GLU and T-BIL in the serum of infected and naive mice were measured. The mean \pm SD of Fe

concentration in the serum of 5 infected C57BL/6 ($273.00 \pm 11.66 \mu\text{g/dL}$) was significantly higher than the naive one ($147.40 \pm 6.65 \mu\text{g/dL}$). The mean \pm SD of Fe concentration in the serum of 5 infected BALB/c ($421.60 \pm 27.50 \mu\text{g/dL}$) was significantly higher than the naive one ($281.60 \pm 14.81 \mu\text{g/dL}$). The mean \pm SD of AST concentration in the serum of 5 infected C57BL/6 ($933.80 \pm 186.76 \text{ IU/L}$) was significantly higher than the naive one ($263.00 \pm 35.50 \text{ IU/L}$). The mean \pm SD of ALT concentration in the serum of 5 infected C57BL/6 ($169.80 \pm 25.59 \text{ IU/L}$) was significantly higher than the naive one ($33.60 \pm 1.50 \text{ IU/L}$). Similarly, The mean \pm SD of ALT concentration in the serum of 5 infected BALB/c ($198.00 \pm 73.01 \text{ IU/L}$) was significantly higher than the naive one ($45.40 \pm 5.46 \text{ IU/L}$). The mean \pm SD of LDH concentration in the serum of 5 infected C57BL/6 ($4604.00 \pm 982.49 \text{ IU/L}$) was significantly higher than the naive one ($592.00 \pm 44.00 \text{ IU/L}$). The mean \pm SD of GLU concentration in the serum of 5 infected BALB/c ($38.60 \pm 14.78 \text{ mg/dL}$) was significantly lower than the naive one ($188.60 \pm 13.54 \text{ mg/dL}$). The mean \pm SD of T-BIL concentration in the serum of 5 infected C57BL/6 ($0.32 \pm 0.087 \text{ mg/dL}$) was significantly higher than the naive one ($0.05 \pm 0.008 \text{ mg/dL}$). Similarly, The mean \pm SD of T-BIL concentration in the serum of 5 infected BALB/c ($0.34 \pm 0.054 \text{ mg/dL}$) was significantly higher than the naive one ($0.07 \pm 0.0058 \text{ mg/dL}$). The concentrations of TP, ALB, BUN, CRE, Na, K, Cl, IP, T-CHO, TG and HDL-C in the serum of infected were rarely different from naive ones. The concentration of Ca and γ -GT in the serum were not

detected [Fig. 5] .

Decreases of weight in C57BL/6

Weight of infected and naive mice was monitored on dpi 0, 2, 4 and 6. On dpi 6, the mean \pm SD of weight of 5 infected C57BL/6 (15.36 ± 0.53 g) was significantly lower than the naive one (20.20 ± 0.80 g). On the other hand, the mean \pm SD of weight of 5 infected BALB/c mice (20.00 ± 0.32 g) was not so different from naive one (21.40 ± 0.68 g) [Fig. 6] .

Decreases of RMBCS score in C57BL/6

RMBCS tests were performed dpi 0, 2, 4 and 6. From dpi 5, a piloerection was occurred in infected mice [Fig. 7] .On dpi 6, the mean \pm SD of RMBCS score of 5 infected C57BL/6 (3.10 ± 3.28) was significantly lower than naive one (18.90 ± 0.10). The mean \pm SD of RMBCS score of 5 infected BALB/c (12.70 ± 2.2) was mildly lower than naive one (17.75 ± 0.19) [Fig. 8] .

Decrease of the number of breaths per minute in C57BL/6

The number of breaths per minute was monitored on dpi 0, 2, 4 and 6. On dpi 6, the mean \pm SD of breaths per minute of 5 infected C57BL/6 (202.67 ± 8.74 times) was significantly lower than the naive one (255.67 ± 0.33 times). On the other hand, the mean \pm SD of breaths per minute of 5 infected BALB/c (247.33 ± 11.67 times) was not so different from naive one ($239 \pm$

8.89 times) [Fig. 9] .

Development of splenomegaly

Mice were sacrificed and performed the autopsy in dpi 6. Sizes of the spleens were significantly larger than those of naive mice, and the color was darker [Fig. 10A] . On dpi 6, the mean \pm SD of spleen weight of 5 infected C57BL/6 (139.00 ± 14.19 mg) was significantly heavier than naive one (56.60 ± 1.96 mg). The mean \pm SD of spleen weight of 5 infected BALB/c (213.00 ± 10.00 mg) was significantly heavier than naive one (77.60 ± 2.33 mg) [Fig. 10B] .

Color alternation of organs and red spots on the skin in C57BL/6

The color of liver and gallbladder in infected C57BL/6 were darker than naive ones. The color of adrenal gland, white in naive C57BL/6, altered to be red. The colors of other organs were not different. Some red spots were observed in the dermis of infected C57BL/6 [Fig. 11] .

1.4 Discussion

This is a first study examined clinical features of *P. berghei* infected mice exhaustively. The parasitemia occurred in both C57BL/6 and BALB/c. Its growth rate was not different among strain [Fig. 3]. The parasitemia rate became high around 60-80% on the day which mice died. (data not shown). It unbelievably higher than one reported in human (White et al., 2013). The level of hematocrit, markedly decreasing in both strain showed that anemia occurred in both strain [Fig. 4]. It was suggested cause by increase of *P. berghei* parasites and broken RBCs. The blood biochemical examinations for screening for dysfunction of brain, liver, gallbladder, kidney, heart and pancreas showed the increase of Fe, ALT and T-BIL. These results suggested liver and gallbladder injury [Fig. 5]. From dpi 5, piloerection was observed in both strain [Fig. 7] but a weight loss occurred only in C57BL/6 ([Fig. 6]. C57BL/6 died on about dpi 7 whereas BALB/c died about dpi 8 (data not shown). These results suggested that state of C57BL/6 became more serious than BALB/c.

RMCBS tests showed that a consciousness and movement disturbance occurred only in C57BL/6 [Fig. 8]. Additionally, decrease of breathing in *P.*

berghei-infected C57BL/6 showed respiration failure [Fig. 9] . The autopsy showed that enormous splenomegaly occurred in both strain [Fig. 10] . The color alternation of spleens and livers indicated deposition of malaria pigment, whose color is dark brown [Fig. 11] . The color of adrenal gland became red and some red spots were observed in the dermis [Fig. 11] These results suggested that abnormal bleeding occurred in *P. berghei*-infected C57BL/6. However brains didn't changed by visual examination. In *P. berghei*-infected C57BL/6, lungs from one became red but other two didn't.

In summary, parasitemia, anemia, splenomegaly, kidney and gallbladder injury occurred in both strains, otherwise consciousness and movement disturbance, respiration failure and abnormal bleeding occurred only C57BL/6. These results indicated that *P. berghei*-infected C57BL/6 had several severe manifestations that weren't occurred in BALB/c even though rate of infection was same [Fig. 12] .

In chapter 2 and 3, I tried to clarify a part of the pathogenesis of these severe manifestations observed only in C57BL/6.

Chapter 2

Cerebral edema in *Plasmodium berghei*-infected C57BL/6 mice.

Abstract

In chapter 2, I focused on the vascular abnormality in the brain to clarify a part of pathogenesis of the consciousness disturbance observed in *P. berghei*-infected C57BL/6 in chapter 1. 1×10^6 *P. berghei* ANKA were inoculated to C57BL/6. The brains were examined on dpi6. In *P. berghei*-infected C57BL/6, Evans blue leaked to cerebral parenchyma. This result showed that BBB breakdown occurred and the permeability of cerebral capillaries was increased. By histochemical examinations, the leakage of RBCs and WBCs was not detected in perivascular space, but IgG leaked to cerebral parenchyma. These results showed that not hemocytes but plasma leaked to cerebral parenchyma and formed cerebral edema. Cerebral edema can impair the action of nerve cells in several ways. In summary, it suggested that hyperpermeability of cerebral capillaries causes cerebral edema and it plays a part of pathogenesis of consciousness disturbance observed *P. berghei*-infected C57BL/6 in chapter 1.

2.1 Introduction

In chapter 2, I focused on the vascular abnormality in the brain to clarify a part of pathogenesis of the consciousness disturbance observed in *P. berghei*-infected C57BL/6 in chapter 1.

Brain

The brain is an organ that serves as the center of the nervous system in animals. It is located in the head, usually close to the primary sensory organs for such senses as vision, hearing, balance, taste, and smell. In the cerebral cortex (the largest part) is estimated to contain numerous neurons, each connected by synapses to several thousand other neurons (Pelvig, Pakkenberg, Stark, & Pakkenberg, 2008). These neurons communicate with one another by means of long protoplasmic fibers called axons, which carry trains of signal pulses called action potentials to distant parts of the brain or body targeting specific recipient cells.

Cerebral organization

The brain could be divide into several regions: the telencephalon (cerebral hemispheres, olfactory bulb), diencephalon (thalamus and hypothalamus

with pineal gland), mesencephalon (midbrain), cerebellum, pons, and medulla (SCHULTZ, 2001). Each region was involved different functions of brain. Visually, the interior of the brain consists of areas of so-called grey matter, with a dark color, separated by areas of white matter, with a lighter color. The brains are surrounded by a system of connective tissue membranes called meninges that separate the skull from the brain. Blood vessels enter the central nervous system through holes in the meningeal layers. The cells in the blood vessel walls are joined tightly to one another, forming the BBB, which blocks the passage of many toxins and pathogens (though at the same time blocking antibodies and some drugs) (Patterson & Schmidt, 2003).

The blood-brain barrier

The brain contains a network of blood vessels which are necessary for providing nutrients, and oxygen, and for removing carbon dioxide and waste. This network of capillaries together with the glia form a protective barrier called the BBB. This barrier prevents large molecules and pathogens in the blood from entering the brain tissues and from altering the brain's functions (Cardoso, Brites, & Brito, 2010; Neuwelt et al., 2011). The brain is very sensitive to blood chemistry variations and its homeostasis is tightly regulated (Levin, Magnan, Dunn-Meynell, & Le Foll, 2011). The BBB is regarded as a part of the neurovascular unit, a concept that stresses a

cross-talk between the different brain components for optimal functions of the brain. Maintenance of homeostasis is principally due to the brain endothelial cells, which are on the luminal side of the BBB and correspond to the actual barrier site. Brain endothelial cells differ from those found in other tissues in many ways. They are attached by tight junctions of high electrical resistance preventing intercellular passage of molecules, and do not contain small openings called slit pores that allow the diffusion of molecules. Thus to reach the brain parenchyma, essential nutrients need to be actively transported by carrier systems to pass through the capillary wall. Brain endothelial cells also have important functions in mediating and regulating the immune response in the nervous system (Miller, 1999). The inner part of the BBB is composed of pericytes, glial cells and astrocytes that essentially shield the capillaries from the neurons. The pericytes by themselves do not contribute to homeostasis for neurological functioning by contributing to and regulating brain endothelial cell phenotype. In particular, endothelial cells are in contact with foot processes of astrocytes. These cellular structures provide an additional barrier protecting neurons from toxic products in the blood. Astrocytes can also form a barrier called the glia limitans at sites where the endothelial barrier is absent, such as the postrema [Fig. 13] .

2.2 Materials and methods

Animals and parasites

All animal procedures in this study were approved by the Committee for Experimental Animals at the University of Tokyo. Eight week-old C57BL/6 female mice were obtained from Japan Clea, Tokyo, Japan, and housed under specific pathogen-free conditions with free access to food and water. *P. berghei* ANKA was used for this study. Malaria parasites were stored as frozen stocks in liquid nitrogen. PRBCs of *P. berghei* ANKA were generated in donor mice inoculated i.p. with frozen stock of parasites.

Experimental infection

To prepare pRBCs, blood was collected from donor mice and mixed well with Citrate-phosphate-dextrose as anticoagulant. The pRBCs were washed two times with HBSS by centrifugation at 400 xg for 5 min. Six mice were infected by i.p. injection of 1×10^6 pRBCs. In three of them, parasitemia was monitored on Giemsa-stained blood smears from the day dpi1 onwards and estimated over 1000 RBCs and Evans blue assay was performed on dpi6. The other three mice were sacrificed and collected their brains for histopathological examinations.

Evans blue assay

Blood vessel permeability on dpi 6 was assessed using the Evans blue assay as reported previously (Nakazawa, 2005). Briefly, mice were injected i.v. with 200 μ l of HBBS–1% Evans blue, sacrificed 1 h later, and perfused intracardially with HBSS. Brains were surgically removed.

HE stain

At dpi 6, infected and naive mice of both strains were euthanized, following which brains were removed rapidly, fixed in 20% neutral buffered formalin, embedded in paraffin and cut into 4 μ m section. Slides were stained with Mayer's hematoxylin solution (WAKO, Osaka, Japan) and eosin solution (MUTO PURE CHEMICALS CO., LTD., Tokyo, Japan)

Immunohistochemistry

Immunohistochemical analyses were performed on 4 μ m paraffin sections of dpi 6 brains. After deparaffinization, sections were incubated with Block Ace (UK-B 80, DAINIPPONSUMITOMOPHARMA, Osaka, Japan). After 10 min incubation the sections for examining the immunohistochemical localization of IgG were incubated with HRP linked goat-anti mouse IgG (MAX-PO 414351, Nichirei, Tokyo, Japan) for overnight. The

immunoreactivity was visualized by a DAB substrate kit (415192F, Nichirei, Tokyo, Japan).

2.3 Results

Course of infection

From dpi 3, pRBC were observed in peripheral blood for the first time, and pRBC rate was elevated over the course of infection. On dpi 6, the mean \pm SD of parasitemia of 3 mice was 39.67 ± 5.37 % [Fig. 14] .

Exudation of Evans blue to cerebral parenchyma

The brains of infected mice were stained massive blue by Evans blue administered i.v. on dpi 6. In one of mouse, Whole brain was stained. In other mice only cerebrum were stained. The brains of naive mice were not stained [Fig. 15] .

No leakage of hemocytes to cerebral parenchyma

The brains removed from mice were cut at the part of frontal cortex in cerebrum and performed histopathological examination. In cerebral cortex of naive mice, maicrovessels were filled with RBCs. In maicrovessels of infected mice, the number of RBCs was decreased and WBCs accumulation was observed. However, the leakage of RBCs and WBCs was not detected in

perivascular space [Fig. 16] .

Exudation of IgG to cerebral parenchyma

In immunohistochemical examination with antibody against IgG, positive reaction was detected not only in vessels but in perivascular space in cerebral parenchyma of all infected mice. The number of vessels which have exudation IgG was very small [Fig. 17] .

2.4 Discussion

The consciousness disturbance in *P. berghei*-infected C57BL/6 seems to arise from several causes. In chapter 2, I focused on the brain to clarify a part of its pathogenesis.

In *P. berghei*-infected C57BL/6, Evans blue leaked to cerebral parenchyma [Fig. 15] . This result showed that BBB breakdown occurred and the permeability of cerebral capillaries was increased. Also only cerebrum was stained, it showed that hyperpermeability occurred in only cerebrum. The leakage of RBCs and WBCs was not detected in perivascular space [Fig. 16] , but IgG, one of plasma components leaked to cerebral parenchyma [Fig. 17] . These results showed that not hemocytes but plasma leaked to cerebral parenchyma and formed cerebral edema. Cerebral edema can impair the action of nerve cells by increasing the internal pressure to nerve cells or inducing the several cytokines (Hunt et al., 2006; John et al., 2008; Maneerat et al., 1999). Additionally, It was reported that IgG leaked from capillaries to parenchyma of organs forms immune complex and impairs other cells (Chadban & Atkins, 2005; Satoh, Kumar, Kanwar, & Reeves, 1995). My results and these reports suggested that the hyperpermeability of capillaries

in cerebral cortex induced a cerebral edema and might caused the consciousness disturbance by impairing nerve cells.

In mice study, several cases of RBCs leakage (ring hemorrhage) and accumulation of WBCs (sequestration) in *P. berghei*-infected C57BL/6 were reported and considered they plays key roles for murine cerebral malaria (Carroll et al., 2010; Nakazawa, 2005). However, in my study, the ring hemorrhage was not observed and sequestration occurred in *P. berghei*-infected BALB/c which didn't have the consciousness disturbance (data not shown). Therefore, my study can raise a question for these hypotheses.

In human some studies about plasma leakage in cerebral malaria were reported. Radioactive-labeled albumin levels were not increased in the CSF after intravenous injection in Thai adult patients during and after coma (Warrell et al., 1986). In another study, albumin levels in the CSF of Vietnamese adult patients with human cerebral malaria were not different from control subjects (Brown et al., 2000). In Malawian children, the levels of albumin in the CSF were not different between children who died vs. those who survived, although they differ from UK adult controls (Combes et al., 2010). When IgG was investigated, higher levels were detected in the CSF of a significant proportion in Thai patients with human cerebral malaria (Chapel et al., 1987). Therefore, leakage of IgG is one of important features observed in *Plasmodium*-infected brain and clarifying the pathogenesis of

cerebral edema in *P. berghei*-infected C57BL/6 is potentially useful for human research.

In summary, it suggested that hyperpermeability of cerebral capillaries causes cerebral edema and it plays a part of pathogenesis of consciousness disturbance observed *P. berghei*-infected C57BL/6 in chapter 1 [Fig. 18] .

Chapter 3

Pulmonary edema in *Plasmodium berghei*-infected C57BL/6 mice.

Abstract

In chapter 3, I focused on the vascular abnormality in the lung to clarify a part of pathogenesis of the respiration failure observed in *P. berghei*-infected C57BL/6 in chapter 1. 1×10^6 *P. berghei* ANKA were inoculated to C57BL/6. The lungs were collected on dpi 6 and examined by HE stain. RBCs accumulated in alveolar capillaries and fluid accumulated in alveolar space. By Evans blue assay, exudation of Evans blue from the vessels was observed. It showed that the permeability of alveolar capillaries was increased. These results suggested that the increase of permeability in alveolar capillaries induce the accumulation of plasma in alveolar space. The plasma in alveolar space could interrupt the exchange of respiratory gases in the lungs. In summary, hyperpermeability of alveolar capillaries causes pulmonary edema and it plays a part of pathogenesis of respiration failure observed *P. berghei*-infected C57BL/6 in chapter 1.

3.1 Introduction

In chapter 3, I focused on the vascular abnormality in the lung to clarify a part of pathogenesis of the respiration failure observed in *P. berghei* infected C57BL/6 in chapter 1.

Lung

The lung is the essential respiration organ in mice. Mice lungs are located in two cavities on either side of the heart. Though similar in appearance, the two are not identical. Both are separated into lobes by fissures, with four lobes on the right and one on the left. Their principal function is to transport oxygen from the atmosphere into the bloodstream, and to release carbon dioxide from the bloodstream into the atmosphere. A large surface area is needed for this exchange of gases which is accomplished by the mosaic of specialized cells that form millions of tiny, exceptionally thin-walled air sacs called alveoli.

Alveoli

The alveoli are located in the respiratory zone of the lungs, at the distal termination of the alveolar ducts and atria. These air sacs are the forming and termination point of the respiratory tract (Margit Pavelka, 2005). Each alveolus is wrapped in a fine mesh of capillaries covering about 70% of its area (Ochs et al., 2004). The alveoli consist of an epithelial layer and extracellular matrix surrounded by capillaries. In some alveolar walls there are pores between alveoli called Pores of Kohn. The alveoli contain some collagen and elastic fibers. The elastic fibers allow the alveoli to stretch as they are filled with air during inhalation. They then spring back during exhalation in order to expel the carbon dioxide-rich air. There are three major cell types in the alveolar wall:(i) Type I (Squamous Alveolar) cells, that form the structure of an alveolar wall, (ii) Type II (Great Alveolar) cells that secrete pulmonary surfactant to lower the surface tension of water and allows the membrane to separate, therefore increasing its capability to exchange gases. Surfactant is continuously released by exocytosis. It forms an underlying aqueous protein-containing hypophase and an overlying phospholipid film composed primarily of dipalmitoyl phosphatidylcholine. (iii) Macrophages that destroy foreign material, such as bacteria (Coales, 2000) [Fig. 19] .

3.2 Materials and methods

Animals and parasites

All animal procedures in this study were approved by the Committee for Experimental Animals at the University of Tokyo. Eight week-old C57BL/6 female mice were obtained from Japan Clea, Tokyo, Japan, and housed under specific pathogen-free conditions with free access to food and water. *P. berghei* ANKA was used for this study. Malaria parasites were stored as frozen stocks in liquid nitrogen. pRBCs of *P. berghei* ANKA were generated in donor mice inoculated i.p. with frozen stock of parasites.

Experimental infection

To prepare pRBCs, blood was collected from donor mice and mixed well with Citrate-phosphate-dextrose as anticoagulant. The pRBCs were washed two times with HBSS by centrifugation at 400 $\times g$ for 5 min. Six mice were infected by i.p. injection of 1×10^6 pRBCs. In three of them, parasitemia was monitored on Giemsa-stained blood smears from the day dpi 1 onwards and estimated over 1000 RBCs and Evans blue assay was performed on dpi 6. The other three mice were sacrificed and collected their lungs for histopathological examinations.

HE stain

At dpi 6, infected and non-infected mice of both strains were euthanized, following which lungs were removed rapidly, fixed in 20% neutral buffered formalin, embedded in paraffin and cut into 4 μ m section. Slides were stained with Mayer's hematoxylin solution and eosin solution.

Evans blue assay

Blood vessel permeability dpi 6 was assessed using the Evans blue assay. Briefly, mice were injected i.v. with 200 μ l of HBBS-1% Evans blue, sacrificed 1 h later, and perfused intracardially with HBSS. Lungs were surgically removed.

3.3 Results

Course of infection

From dpi 3, pRBC were observed in peripheral blood for the first time, and pRBC rate was elevated over the course of infection. On dpi6, the mean \pm SD of parasitemia of 3 mice was 39.13 ± 1.87 % [Fig. 20] .

RBCs accumulation in alveolar capillaries and fluid accumulation in alveolar space

The lungs removed from mice were cut at the left lobe and performed histopathological examination. In lungs of infected mice, RBCs accumulation was observed in alveolar capillaries and the region of alveolar wall was extended. Some parts of alveolar space were stained with eosin in lungs of infected [Fig. 21] .

Exudation of Evans blue from the vessels

The lungs of infected mice were stained deeply by Evans blue administered intravenously on dpi 6. The lungs of naive mice were not stained [Fig. 22] .

3.4 Discussion

The respiration failure in *P. berghei*-infected C57BL/6 seems to arise from several causes. In chapter 3, I focused on the lung to clarify a part of its pathogenesis.

In *P. berghei*-infected C57BL/6, RBCs accumulation was observed in alveolar capillaries and the region of alveolar wall was extended. Some parts of alveolar space were stained with eosin in lungs of infected [Fig. 21] . These results showed that RBCs made a blood stasis induces internal pressure in alveolar capillaries and fluid accumulation alveolar space. A lot of WBCs were also accumulated in alveolar capillaries. It means that inflammation occurred in lungs with *P. berghei* infection. By Evans blue assay, exudation of Evans blue from the vessels were observed [Fig. 22] . It showed that the permeability of alveolar capillaries was increased. These results suggested that the increase of permeability in alveolar capillaries induce the accumulation of plasma in alveolar space. The plasma in alveolar space could interrupt the exchange of respiratory gases in the lungs. To obtain more oxygen, the breath of mice was suggested to become deeply and decrease its frequency. There are few reports about lungs in *P.*

berghei-infected mice and researchers' opinion divided into two that *P. berghei*-infected C57BL/6 has pulmonary edema or not (Anidi et al., 2013; Epiphanio et al., 2010; Hee et al., 2011). In human, there are a lot of cases of deep breathing and respiratory distress with *P. falciparum* infection (Epiphanio et al., 2010). In previous work in my laboratory, fluid accumulation in alveolar space was observed in HE section from *P. falciparum*-infected patients from Thailand (data not shown). Therefore, pulmonary edema is one of important features observed in *Plasmodium*-infected lungs and clarifying the pathogenesis of pulmonary edema in *P. berghei*-infected C57BL/6 is potentially useful for human research.

In summary, it suggested that hyperpermeability of alveolar capillaries causes pulmonary edema and it plays a part of pathogenesis of respiration failure observed *P. berghei*-infected C57BL/6 in chapter 1 [Fig. 23] .

Chapter 4

Stillbirth with dynamic structural change of placenta occurred in
Plasmodium berghei-infected pregnant C57BL/6 mice.

Abstract

The placenta is a unique, autonomous and a transient organ which is responsible for maternal-fetal exchanges. *P. berghei* infection occurred several severe manifestations in adult C57BL/6 but the effect of maternal *P. berghei* infection to babies and placenta is poorly understood. In this study, first I examined the effects of maternal *P. berghei* infection to babies. 1×10^7 , 10^6 and 10^5 *P. berghei* ANKA were inoculated to pregnant C57BL/6 at G13 (the day on which a vaginal plug was observed in timed mated mice was considered as gestation day one; G1). Viability and weight of babies from *P. berghei*-infected mothers were decreased. Next, I examined the pathological changes of placenta in 1×10^7 *P. berghei*-infected pregnant C57BL/6. At G18, fetuses of infected mice were all dead. In the placenta of infected mice, the junctional zone penetrated abnormally into the labyrinth zone and erythrocytes accumulated in the junctional zone. The number of cytotrophoblast cells was decreased in placental labyrinth zone. Syncytiotrophoblast cells were destructed and maternal red blood space was extended. These findings suggest that maternal *Plasmodium* infection links dynamic structural changes of placenta. Especially, destruction of labyrinth trophoblast cells that divide maternal blood space and fetus blood space provides the potential for the change of blood stream in mother and could be one of causes for fetal damages.

4.1 Introduction

In chapter 4, I focused on the vascular abnormality in the placenta involved in viability of babies.

Function of placenta

The placenta is a unique, autonomous and transient organ which is responsible for maternal-fetal exchanges and maternal tolerance of fetopaternal antigens (Rossant & Cross, 2001). The placenta plays a crucial role in the development of maternal preeclampsia and fetal intrauterine growth restriction (IUGR) (Myatt, 2002) .

Placental development of mice

during the 19-20 days of gestation in mice, placentation evolves from an initially choriovitelline pattern to a chorioallantoic pattern at G12. During the first stage of placentation, the trophoctoderm differentiates in two pathways: (i) polar trophoblastic cells displaying rapid proliferation, giving rise to the extraembryonic ectoderm and ectoplacental cone; and (ii) mural trophoblastic cells that do not divide but instead continue to endoreplicate

their DNA, forming primary trophoblastic giant cells. Meanwhile, the endoderm differentiates within the inner cell mass of the embryo. Parietal endoderm cells migrate onto the basal surface of the trophoblast layer and deposit an extensive basement membrane (Reichert membrane) between the trophoblast giant cells and the parietal endoderm. This first placental structure-the parietal yolk sac- absorbs nutrients from the maternal blood via capillary channels in the decidual tissue that gradually form sinuses between the primary trophoblastic giant cells and the Reichert membrane. On G8, mesoderm cells from the embryo migrate to the inner surface of the visceral endoderm and give rise to the first vascular cells and primitive vitelline vessels (visceral yolk sac). At this stage, nutrient exchanges are ensured by this vascularized zone. These mesodermal cells also form the allantoic mesenchyme, which develops and enters into contact with the chorion of the ectoplacental cone on G9-10. In the chorioallantoic placenta, the allantoic mesoderm gradually invades trophoblastic cells and establishes a network of fetal blood vessels in the developing labyrinthine zone. By G13, the definitive chorioallantoic placenta is clearly subdivided into: (i) a layer of maternal decidua; (ii) a junctional zone; and (iii) a labyrinthine zone. The maternal decidua comprises mesometrial decidual cells and large granular lymphocytes. The junctional zone is limited on the maternal side by a layer of trophoblastic giant cells. The mouse junctional zone also includes two types of cytotrophoblast: (i) spongiotrophoblasts with an eosinophilic

cytoplasm; and (ii) trophoblastic glycogen cells. The trophoblastic glycogen cells decrease in number in this zone late in gestation, progressively invading the decidua. In mice, trophoblastic glycogen cells do not begin to invade the decidua basalis until G13, which is relatively late in gestation; the invasion process is not completed until G15 to G18. Furthermore, trophoblastic invasion in mice does not extend into the myometrium (Enders and Welsh, 1993) and endovascular invasion is very limited. The labyrinth develops from the trophoblast and its associated fetal blood vessels. In the labyrinth, the trophoblast begins to differentiate into three layers: two syncytiotrophoblast layers in contact with the fetal endothelium, and one cytotrophoblast layer in contact with maternal blood. Therefore, three trophoblast layers separate the maternal blood from the fetal blood; this type of placental development is known as haemotrichorial placentation (Enders & Welsh, 1993). In syncytiotrophoblast cells, Syncytin-A, an endogenous retroviral envelope protein is expressed and is involved in fusion of the cytotrophoblast cells to form the multinucleated syncytial layer of the placenta (Dupressoir et al., 2009) .

The maternal blood supply crosses the spongiotrophoblast layer via arterial sinuses in which the endothelial cells have been replaced by spongiotrophoblast cell. The maternal blood then enters the labyrinth and bathes the fetal trophoblast, allowing exchanges with fetal blood (Georgiades, Ferguson-Smith, & Burton, 2002; Müntener & Hsu, 1977) In mice, the

definitive structure of the placenta is therefore completed halfway through gestation, and trophoblast invasion occurs late in gestation, in a spatially and temporally discrete manner [Fig. 24] .

4.2 Materials and methods

Animals and parasites

All animal procedures in this study were approved by the Committee for Experimental Animals at the University of Tokyo. Eight to thirteen week-old C57BL/6 female mice were obtained from Japan Clea, Tokyo, Japan, and housed under specific pathogen-free conditions with free access to food and water. *P. berghei* ANKA was used for this study. Malaria parasites were stored as frozen stocks in liquid nitrogen. pRBCs of *P. berghei* ANKA were generated in donor mice inoculated i.p. with frozen stock of parasites.

Gestation timing and pregnancy monitoring

Detection of the vaginal plug and measurement of body weight were jointly used to time gestation, as described by Neres and Penha (Neres, Marinho, Gonçalves, Catarino, & Penha-Gonçalves, 2008). Two to three females were put together with one male for 2 days, and examined for the presence of vaginal plug every morning. The day on which a vaginal plug was observed in timed mated mice was considered as gestation day one (G1) and pregnancy progression was monitored every day by weighting the females. Successful fertilization was confirmed between G10 and G13 when the

animals had an average increase of 3–4 g in body weight. Thus, weight gain was taken as sign of pregnancy and abrupt weight loss as indicator of pregnancy damage or interruption.

Experimental infection

To prepare pRBCs, blood was collected from donor mice and mixed well with Citrate-phosphate-dextrose as anticoagulant. The pRBCs were washed two times with HBSS by centrifugation at 400 xg for 5 min. First trial, pregnant mice were infected at G13 with 1×10^7 , 10^6 and 10^5 pRBCs (n=2). Parasitemia and maternal weight were monitored. On G17-G20, newborns after birth were collected and examined their viability. Newborns who had whole body were weighted. Second trial, pregnant mice were infected at G13 with 1×10^7 pRBCs (n=3). Parasitemia was monitored on Giemsa-stained blood smears from the dpi1 onwards and estimated over 2000 RBCs. On G18, caesarean section was performed and evaluated pregnancy outcome.

Fetal survival and weight evaluation

On G18, pregnant females were sacrificed, the uterus was examined and the number of fetuses and resorptions were recorded. Resorptions were identified as small implants with no discernible fetus and placenta, corresponding to embryos that died before complete placenta vascularization. The fetuses were extracted from their amniotic envelope and viability was

immediately evaluated by prompted movement reaction to touching with pliers. The lack of reactive movement indicated that the fetus had recently died and was considered a stillborn. Babies born before G18 were identified premature. Fetuses and placentas were separately weighted. After examination, living fetuses were euthanized.

HE stain

At G18, infected and naive mice of both strains were euthanized, following placentae were removed rapidly, fixed in 20% neutral buffered formalin, embedded in paraffin and cut into 4 μm section. Slides were stained with Mayer's hematoxylin solution and eosin solution.

Immunohistochemistry

Immunohistochemical analyses were performed on 4 μm paraffin sections of G18 placentae. After deparaffinization, sections were immersed in 0.3% (v/v) hydrogen peroxidase/methanol for quenching endogenous peroxidase. After 10 min incubation with Block Ace, the sections for examining the immunohistochemical localization of syncytin were incubated with polyclonal rabbit anti-human syncytin antibody (sc-50369, Santa Cruz Biotechnology, Inc., Texas, USA) for 60 min at room temperature. After being washed with PBS, they were incubated with HRP linked donkey anti-rabbit IgG antibody (NA9340, Amersham, Buckinghamshire, UK) at room

temperature for 30min. The immunoreactivity was visualized by the DAB substrate kit.

Statistical analysis

Statistical analyses were performed by *t*-test, and *p* values less than 0.01 were considered statistically significant.

4.3 Results

Decrease survival rate and weight of newborns from infected mother.

Newborns after birth from pRBCs-infected mothers were examined their viability and weight. The mortality rate of newborns from pRBCs-infected mother was higher than naive one and it depended on amount of inoculated pRBCs. The mean of mortality rate of newborns from 10^7 pRBCs-infected mothers was 100% (n=2). The mean of mortality rate of newborns from 10^6 pRBCs-infected mothers was 64.71% (n=2). The mean of mortality rate of newborns from 10^5 pRBCs-infected mothers was 21.05%(n=2). On the other hand, the mean of mortality rate of newborns from naive mothers was 15% (n=2). The weight of newborns from pRBCs-infected mothers was lower than naive one and it depended on amount of inoculated pRBCs. The mean \pm SD of weight of newborns from 10^7 pRBCs-infected mothers was 0.76 ± 0.022 g (n=5). The mean \pm SD of weight of newborns from 10^6 pRBCs-infected mothers was 0.98 ± 0.018 g (n=14). The mean \pm SD of weight of newborns from 10^5 pRBCs-infected mothers was 1.18 ± 0.024 g (n=16). On the other hand, the mean \pm SD of weight of newborns from naive mother was 1.26 ± 0.032 g (n=20) [Fig. 25] .

Increase of pRBCs and decrease maternal weight in 10^7 pRBCs-infected mothers

From G15 (dpi 2), pRBCs were observed in peripheral blood for the first time, and parasitemia was elevated over the course of infection. On G18 (dpi 5), the mean \pm SD of parasitemia of 3 mice was $46.93 \pm 11.31\%$. The parasitemia of pregnant mice tended to be severer than non-pregnant one ($34.93 \pm 3.05\%$, on dpi 5) [Fig. 26A] . Maternal weight of infected mice decreased from G17 (dpi 4). On G18 was the weight of infected mother (30.67 ± 0.88 g) significantly lower than the weight of naive mother (39.67 ± 1.86 g) [Fig. 26B] .

Pregnancy outcome of 10^7 pRBCs-infected mothers

Pregnancy outcome obtained caesarean section on G18. Fetuses from 10^7 pRBCs-infected mothers were all dead [Fig. 27, Table 2] . The number of resorptions, identified as small implants with no discernible fetus and placenta, were higher than the naive one. Premature was observed in 10^7 pRBCs-infected mothers. The mean \pm SD of weight of fetuses from infected mothers (0.70 ± 0.07 g) was lower than naive one (0.78 ± 0.093 g). The mean \pm SD of weight of placentae from infected mother (0.114 ± 0.026 g) was higher than naive one (0.083 ± 0.012 g).

Penetration of junctional zone and RBCs accumulation in junctional zone

On G18 (dpi 5), the placentae were removed from 10^7 pRBCs-infected mothers and performed HE stain. In placenta of infected mother, the junctional zone penetrated abnormally into the labyrinth zone [Fig. 28] . RBCs accumulated in junctional zone, especially outer edges of placenta [Fig. 29A] . Some cells had two nuclei and their cytoplasm was stained deeper by eosin than naive one [Fig. 29A] .

Decrease of cytotrophoblast cells and destruction of syncytiotrophoblast cells in labyrinth zone

On G18 (dpi 5), the placentae were removed from 10^7 pRBCs-infected mothers and performed HE stain. In labyrinth zone of infected mother, the number of cytotrophoblast cells was lower than naive one. In immunohistochemical examination with antibody against syncytin expressed only syncytiotrophoblast cells, the part which had positive reaction was decreased and the gap space was extended. These results indicated the syncytiotrophoblast cells were destructed and maternal and fetal blood space were extended [Fig. 30] .

4.4 Discussion

It was showed that maternal *P. berghei* infection had harmful effects to babies' viability or weight and caused stillbirth and low birth weight [Fig. 25] Some cases of stillbirth or low birth weight with *Plasmodium* infection were already reported in mice but I first clarified the babies loss occurred depend on the number of *P. berghei* infected to mother. Interestingly enough, baby loss did not depend on parasitemia with maternal *P. chabaudi* infection (data not shown). It is suggested that there are a lot of causes for baby loss and the cause are different among *Plasmodium* parasites. Additionally, many epidemiological researches indicated that maternal *Plasmodium* infection causes pregnancy loss in human. Each year more than 125 million pregnant women are at risk of malaria infection, which can have serious consequences for them and their offspring, especially in first- and second-time mothers (Dellicour, Tatem, Guerra, Snow, & ter Kuile, 2010) . In highly endemic settings up to 50% of low birth weight deliveries can be attributed to malaria in pregnancy, leading to approximately 100,000 infant deaths annually, many of which are consequences of IUGR (Desai et al., 2007). Therefore pregnancy women were included risk group along with young children and HIV/AIDS patients (Umbers, Aitken, & Rogerson, 2011). Therefore, to clarify the mechanism of babies loss with maternal *P.*

berghei infection is potentially useful for human research.

It was showed that placental dynamic structural changes occurred when fetuses died with *P. berghei* infection. Maternal RBCs accumulated in junctional zone [Fig. 29] . It suggested that maternal RBCs finished supplying nutrients and oxygen to fetus made a blood stasis causing the maternal blood circulation disorder. This is first report the RBCs accumulation in junctional zone. Some cases of RBCs accumulation in labyrinth zone were reported in *P. berghei* infected mice (Neres et al., 2008; Sharma, Kaur, & Shukla, 2012). The spongiotrophoblast cells proliferated abnormally [Fig. 29B] and the junctional zone was extended and penetrated to labyrinth zone [Fig. 28] The thickened junctional zone was reported in rats with low oxygen environment (Rosario, Konno, & Soares, 2008). Also Brown Norway rats, having a thin junctional zone is very sensitive with hypoxic stress (Konno, Rempel, Arroyo, & Soares, 2007). These results and reports suggested that low oxygen stress arising from maternal *P. berghei* infection induces proliferation and invasion of spongiotrophoblast cells toward fetal side. Additionally these results support that placental structural change observed in this study didn't occur after fetal death.

It was showed that cytotrophoblast cells were disappeared and syncytiotrophoblast layer was destructed [Fig. 30, Fig. 31] . These results suggested that breakdown of placental barrier occurred. The

syncytiotrophoblast layer plays a key role for maternal immune tolerance by lack of expression of MHC antigens (Murphy & Tomasi, 1998). If permeability of placenta barrier is changed, not only the poor nutrient supply but also the failure of the maternal immune tolerance system was occurred and cause to fetal death. There are a few report of placental syncytiotrophoblast cells were destructed when the women had *Plasmodium falciparum* infection (Crocker et al., 2004). Also in vitro study, it was reported that malaria pigment impaired the human trophoblast cells (Lucchi et al., 2011) . Research of placenta and fetus of human during pregnancy is very difficult because of its ethically problem. In addition, the placental structure of human is really similar to mice (they are classified same group of hemochorial placenta). Therefore, to clarify the mechanism of placental structure change with maternal *P. berghei* infection is potentially useful for human research.

In summary, it suggested that the dynamic placental structure change triggered the change of permeability of placental barrier and it plays a part of pathogenesis of fetal death in maternal *P. berghei* infection [Fig. 32] .

General conclusion

Plasmodium is a genus of parasitic protozoa. Infection with *Plasmodium* parasites is known as malaria. However, the pathogenesis of *Plasmodium* infection is poorly understood. In this study, I focused on the one of hosts, mice, which can be used established experimental infection. In chapter 1, I designed objective of this study to reveal what kind of manifestations occurred in *P. berghei*-infected C57BL/6 and BALB/c. 1×10^6 *P. berghei* ANKA were inoculated to C57BL/6 and BALB/c. I performed the blood examination, consciousness and movement test, and autopsy. The parasitemia occurred in both C57BL/6 and BALB/c. Its growth rate was not different among strain. Anemia, splenomegaly, liver and gallbladder injury occurred in both strains. On the other hand, consciousness and movement disturbance, respiration failure and abnormal bleeding occurred only in *P. berghei*-infected C57BL/6. These results indicated that *P. berghei*-infected C57BL/6 had several severe manifestations that weren't occurred in BALB/c even though rate of infection was same.

In chapter 2, I focused on the vascular abnormality in the brain to clarify a part of pathogenesis of the consciousness disturbance observed in *P. berghei*-infected C57BL/6 in chapter1. 1×10^6 *P. berghei* ANKA were inoculated to C57BL/6. The brains were examined on dpi6. In *P.*

berghei-infected C57BL/6, Evans blue leaked to cerebral parenchyma. This result showed that BBB breakdown occurred and the permeability of cerebral capillaries was increased. By histochemical examinations, the leakage of RBCs and WBCs was not detected in perivascular space, but IgG leaked to cerebral parenchyma. These results showed that not hemocytes but plasma leaked to cerebral parenchyma and formed cerebral edema. Cerebral edema can impair the action of nerve cells in several ways. In summary, it suggested that hyperpermeability of cerebral capillaries causes cerebral edema and it plays a part of pathogenesis of consciousness disturbance observed *P. berghei*-infected C57BL/6 in chapter 1.

In chapter 3, I focused on the vascular abnormality in the lung to clarify a part of pathogenesis of the respiration failure observed in *P. berghei*-infected C57BL/6 in chapter 1. 1×10^6 *P. berghei* ANKA were inoculated to C57BL/6. The lungs were collected on dpi6 and examined by HE stain. RBCs accumulated in alveolar capillaries and fluid accumulated in alveolar space. By Evans blue assay, exudation Evans blue from the vessels was observed. It showed that the permeability of alveolar capillaries was increased. These results suggested that the increase of permeability in alveolar capillaries induce the accumulation of plasma in alveolar space. The plasma in alveolar space could interrupt the exchange of respiratory gases in the lungs. In summary, hyperpermeability of alveolar capillaries causes pulmonary edema and it plays a part of pathogenesis of respiration failure observed *P.*

berghei-infected C57BL/6 in chapter 1.

In chapter 4, I focused on placenta. The placenta is a unique, autonomous and transient organ, which is responsible for maternal-fetal exchanges. *P.berghei*-infection occurred several severe manifestations in adult C57BL/6 but the effect of maternal *P. berghei* infection to babies and placenta is poorly understood. In chapter 4, first I examined the effects of maternal *P. berghei* infection to babies. 1×10^7 , 10^6 and 10^5 *P. berghei* ANKA were inoculated to pregnant C57BL/6 at G13. Viability and weight of babies from *P. berghei*-infected mothers were decreased. Next, I examined the pathological changes of placenta in 1×10^7 *P. berghei*-infected pregnant C57BL/6. On G18, fetuses of infected mice were all dead. In the placenta of infected mice, the junctional zone penetrated abnormally into the labyrinth zone and erythrocytes accumulated in the junctional zone. The number of cytotrophoblast cells was decreased in placental labyrinth zone. Syncytiotrophoblast cells were destructed and maternal red blood space was extended. These findings suggest that maternal *Plasmodium* infection links dynamic structural changes of placenta. Especially, destruction of labyrinth trophoblast cells that divide maternal blood space and fetus blood space provides the potential for the changes of permeability of placenta and the blood stream in mother and could be one of causes for fetal damages.

In general conclusion, *P. berghei*-infected C57BL/6 has several severe manifestations and the change of vessel permeability plays a part of

pathogenesis of them in common [Fig. 33]. It can provide a new explanation of pathogenesis of *Plasmodium* infection. Furthermore, some parts of these manifestations in mice mimic human manifestations with *P. falciparum* infection. Therefore, to clarify the pathological mechanism of these severe manifestations in mice is potentially useful for human research.

Acknowledgements

I'd like to express sincere appreciation to Prof. Yoshitsugu Matsumoto. My theses would not have been completed without his guidance and appropriate advice.

Special appreciation is offered to my advisor, Dr. Yasuyuki Goto and Dr. Chizu Sanjoba for their helpful advice and patient teaching of the protocols used in present investigation.

Special appreciation is offered to Dr. Toshihiro Konno for his helpful advice.

Special appreciation is offered to Assoc. Prof. Kazuhiko Imakawa and Dr. Toshihiro Sakurai for generously providing some antibodies.

Appreciation is also extended to Yasutaka Osada, Haruka Mizobuchi, and Shoko Isokawa for their help my examinations.

I wish to express my special thanks to all members of Laboratory of Molecular immunology, Graduate School of Agriculture and Life Sciences, the University of Tokyo.

Lastly, I'd like to express sincere gratitude to my family for their understanding and support.

References

- Anidi, I. U., Servinsky, L. E., Rentsendorj, O., Stephens, R. S., Scott, A. L., & Pearse, D. B. (2013). CD36 and Fyn Kinase Mediate Malaria-Induced Lung Endothelial Barrier Dysfunction in Mice Infected with *Plasmodium berghei*. *PloS one*, *8*, e71010.
doi:10.1371/journal.pone.0071010
- Atkinson, C. T., & Samuel, M. D. (2010). Avian malaria *Plasmodium relictum* in native Hawaiian forest birds: epizootiology and demographic impacts on 'apapane *Himatione sanguinea*. *Journal of Avian Biology*, *41*, 357–366. doi:10.1111/j.1600-048X.2009.04915.x
- Brown, H. C., Chau, T. T., Mai, N. T., Day, N. P., Sinh, D. X., White, N. J., ... Turner, G. D. (2000). Blood-brain barrier function in cerebral malaria and CNS infections in Vietnam. *Neurology*, *55*, 104–111.
doi:10.1212/WNL.55.1.104
- Cardoso, F. L., Brites, D., & Brito, M. A. (2010). Looking at the blood-brain barrier: molecular anatomy and possible investigation approaches. *Brain research reviews*, *64*, 328–363.
doi:10.1016/j.brainresrev.2010.05.003
- Carroll, R. W., Wainwright, M. S., Kim, K.-Y., Kidambi, T., Gómez, N. D., Taylor, T., & Haldar, K. (2010). A rapid murine coma and behavior scale for quantitative assessment of murine cerebral malaria. *PloS one*, *5*.
doi:10.1371/journal.pone.0013124

- Ceneviva, A. C., & Camargo, M. E. (1979). Plasmodium gallinaceum-parasitized chicken erythrocytes in a practical hemagglutination test for IgM antibodies in human malaria. *The American journal of tropical medicine and hygiene*, *28*, 622–626.
- Chadban, S. J., & Atkins, R. C. (2005). Glomerulonephritis. *Lancet*, *365*, 1797–806. doi:10.1016/S0140-6736(05)66583-X
- Chang, K.-H., & Stevenson, M. M. (2004). Malarial anaemia: mechanisms and implications of insufficient erythropoiesis during blood-stage malaria. *International journal for parasitology*, *34*, 1501–1516. doi:10.1016/j.ijpara.2004.10.008
- Chapel, H. M., Warrell, D. A., Looareesuwan, S., White, N. J., Phillips, R. E., Warrell, M. J., ... Tharavanij, S. (1987). Intrathecal immunoglobulin synthesis in cerebral malaria. *Clinical and experimental immunology*, *67*, 524–530.
- Coales, P. (2000). Principles of Anatomy and Physiology. *Physiotherapy*. doi:10.1016/S0031-9406(05)60992-3
- Collins, W. E., Skinner, J. C., Broderson, J. R., Filipski, V. K., Morris, C. M., Stanfill, P. S., & Warren, M. (1992). Susceptibility of Macaca fascicularis monkeys from Mauritius to different species of Plasmodium. *The Journal of parasitology*, *78*, 505–511. doi:Doi 10.2307/3283652
- Combes, V., El-Assaad, F., Faille, D., Jambou, R., Hunt, N. H., & Grau, G. E. R. (2010). Microvesiculation and cell interactions at the brain-endothelial interface in cerebral malaria pathogenesis. *Progress in neurobiology*, *91*, 140–151. doi:10.1016/j.pneurobio.2010.01.007

- Crocker, I. P., Tanner, O. M., Myers, J. E., Bulmer, J. N., Walraven, G., & Baker, P. N. (2004). Syncytiotrophoblast degradation and the pathophysiology of the malaria-infected placenta. *Placenta*, *25*, 273–282. doi:10.1016/j.placenta.2003.09.010
- Dellicour, S., Tatem, A. J., Guerra, C. A., Snow, R. W., & ter Kuile, F. O. (2010). Quantifying the number of pregnancies at risk of malaria in 2007: a demographic study. *PLoS medicine*, *7*, e1000221. doi:10.1371/journal.pmed.1000221
- Desai, M., ter Kuile, F. O., Nosten, F., McGready, R., Asamo, K., Brabin, B., & Newman, R. D. (2007). Epidemiology and burden of malaria in pregnancy. *The Lancet infectious diseases*, *7*, 93–104. doi:10.1016/S1473-3099(07)70021-X
- Dupressoir, A., Vernochet, C., Bawa, O., Harper, F., Pierron, G., Opolon, P., & Heidmann, T. (2009). Syncytin-A knockout mice demonstrate the critical role in placentation of a fusogenic, endogenous retrovirus-derived, envelope gene. *Proceedings of the National Academy of Sciences of the United States of America*, *106*, 12127–12132. doi:10.1073/pnas.0902925106
- Enders, A. C., & Welsh, A. O. (1993). Structural interactions of trophoblast and uterus during hemochorial placenta formation. *The Journal of experimental zoology*, *266*, 578–587. doi:10.1002/jez.1402660608
- Epiphany, S., Campos, M. G., Pamplona, A., Carapau, D., Pena, A. C., Ataíde, R., ... Mota, M. M. (2010). VEGF promotes malaria-associated acute lung injury in mice. *PLoS pathogens*, *6*, e1000916. doi:10.1371/journal.ppat.1000916

- Georgiades, P., Ferguson-Smith, A. C., & Burton, G. J. (2002). Comparative developmental anatomy of the murine and human definitive placentae. *Placenta*, *23*, 3–19. doi:10.1053/plac.2001.0738
- Hee, L., Dinudom, A., Mitchell, A. J., Grau, G. E., Cook, D. I., Hunt, N. H., & Ball, H. J. (2011). Reduced activity of the epithelial sodium channel in malaria-induced pulmonary oedema in mice. *International journal for parasitology*, *41*, 81–88. doi:10.1016/j.ijpara.2010.07.013
- Hunt, N. H., Golenser, J., Chan-Ling, T., Parekh, S., Rae, C., Potter, S., ... Ball, H. J. (2006). Immunopathogenesis of cerebral malaria. *International journal for parasitology*, *36*, 569–582. doi:10.1016/j.ijpara.2006.02.016
- John, C. C., Panoskaltis-Mortari, A., Opoka, R. O., Park, G. S., Orchard, P. J., Jurek, A. M., ... Boivin, M. J. (2008). Cerebrospinal fluid cytokine levels and cognitive impairment in cerebral malaria. *The American journal of tropical medicine and hygiene*, *78*, 198–205.
- Konno, T., Rempel, L. A., Arroyo, J. A., & Soares, M. J. (2007). Pregnancy in the brown Norway rat: a model for investigating the genetics of placentation. *Biology of reproduction*, *76*, 709–718. doi:10.1095/biolreprod.106.056481
- Levin, B. E., Magnan, C., Dunn-Meynell, A., & Le Foll, C. (2011). Metabolic sensing and the brain: who, what, where, and how? *Endocrinology*, *152*, 2552–2557. doi:10.1210/en.2011-0194
- Lucchi, N. W., Sarr, D., Owino, S. O., Mwalimu, S. M., Peterson, D. S., & Moore, J. M. (2011). Natural hemozoin stimulates syncytiotrophoblast to secrete chemokines and recruit peripheral blood mononuclear cells. *Placenta*, *32*, 579–585. doi:10.1016/j.placenta.2011.05.003

- Mackinnon, M. J., Gaffney, D. J., & Read, A. F. (2002). Virulence in rodent malaria: host genotype by parasite genotype interactions. *Infection, genetics and evolution : journal of molecular epidemiology and evolutionary genetics in infectious diseases*, *1*, 287–296.
doi:10.1016/S1567-1348(02)00039-4
- Maneerat, Y., Pongponratn, E., Viriyavejakul, P., Punpoowong, B., Looareesuwan, S., & Udomsangpetch, R. (1999). Cytokines associated with pathology in the brain tissue of fatal malaria. *The Southeast Asian journal of tropical medicine and public health*, *30*, 643–649.
- Margit Pavelka, J. R. (2005). *Functional Ultrastructure An Atlas of Tissue Biology and Pathology. Parasitology international* (Vol. 59, pp. 539–48).
doi:10.1016/j.parint.2010.07.001
- Miller, D. W. (1999). Immunobiology of the blood-brain barrier. *Journal of neurovirology*, *5*, 570–578. doi:10.3109/13550289909021286
- Müntener, M., & Hsu, Y. C. (1977). Development of trophoblast and placenta of the mouse. A reinvestigation with regard to the in vitro culture of mouse trophoblast and placenta. *Acta anatomica*, *98*, 241–252.
doi:10.1159/000144801
- Murphy, S. P., & Tomasi, T. B. (1998). Absence of MHC class II antigen expression in trophoblast cells results from a lack of class II transactivator (CIITA) gene expression. *Molecular reproduction and development*, *51*, 1–12.
doi:10.1002/(SICI)1098-2795(199809)51:1<1::AID-MRD1>3.0.CO;2-L
- Myatt, L. (2002). Role of placenta in preeclampsia. *Endocrine*, *19*, 103–111.
doi:10.1385/ENDO:19:1:103

- Nakazawa, S. (2005). Plasmodium berghei NK65: studies on the effect of treatment duration and inoculum size on recrudescence. *Experimental parasitology*, *111*, 59–63. doi:10.1016/j.exppara.2005.05.002
- Neres, R., Marinho, C. R. F., Gonçalves, L. A., Catarino, M. B., & Penha-Gonçalves, C. (2008). Pregnancy outcome and placenta pathology in Plasmodium berghei ANKA infected mice reproduce the pathogenesis of severe malaria in pregnant women. *PloS one*, *3*, e1608. doi:10.1371/journal.pone.0001608
- Neuwelt, E. A., Bauer, B., Fahlke, C., Fricker, G., Iadecola, C., Janigro, D., ... Drewes, L. R. (2011). Engaging neuroscience to advance translational research in brain barrier biology. *Nature reviews. Neuroscience*, *12*, 169–182. doi:10.1038/nrn2995
- Ochs, M., Nyengaard, J. R., Jung, A., Knudsen, L., Voigt, M., Wahlers, T., ... Gundersen, H. J. G. (2004). The number of alveoli in the human lung. *American journal of respiratory and critical care medicine*, *169*, 120–124. doi:10.1164/rccm.200308-1107OC
- Pasvol, G. (2005). Management of severe malaria: interventions and controversies. *Infectious disease clinics of North America*, *19*, 211–240. doi:10.1016/j.idc.2004.10.007
- Patterson, D. W., & Schmidt, L. A. (2003). Neuroanatomy of the human affective system. *Brain and cognition*, *52*, 24–26. doi:10.1016/S0278-2626(03)00005-8
- Pelvig, D. P., Pakkenberg, H., Stark, A. K., & Pakkenberg, B. (2008). Neocortical glial cell numbers in human brains. *Neurobiology of aging*, *29*, 1754–1762. doi:10.1016/j.neurobiolaging.2007.04.013

- Penet, M.-F., Kober, F., Confort-Gouny, S., Le Fur, Y., Dalmaso, C., Coltel, N., ... Viola, A. (2007). Magnetic resonance spectroscopy reveals an impaired brain metabolic profile in mice resistant to cerebral malaria infected with *Plasmodium berghei* ANKA. *The Journal of biological chemistry*, *282*, 14505–14514. doi:10.1074/jbc.M608035200
- Rosario, G. X., Konno, T., & Soares, M. J. (2008). Maternal hypoxia activates endovascular trophoblast cell invasion. *Developmental biology*, *314*, 362–375. doi:10.1016/j.ydbio.2007.12.007
- Rossant, J., & Cross, J. C. (2001). Placental development: lessons from mouse mutants. *Nature reviews. Genetics*, *2*, 538–548. doi:10.1038/35080570
- Salakij, J., Lertwatcharasarakul, P., Kasorndorkbua, C., & Salakij, C. (2012). *Plasmodium circumflexum* in a Shikra (*Accipiter badius*): phylogeny and ultra-structure of the haematozoa. *The Japanese journal of veterinary research*, *60*, 105–9. Retrieved from <http://www.ncbi.nlm.nih.gov/pubmed/23094585>
- Satoh, M., Kumar, A., Kanwar, Y. S., & Reeves, W. H. (1995). Anti-nuclear antibody production and immune-complex glomerulonephritis in BALB/c mice treated with pristane. *Proceedings of the National Academy of Sciences of the United States of America*, *92*, 10934–10938. doi:10.1073/pnas.92.24.10934
- SCHULTZ, S. K. (2001). Principles of Neural Science, 4th ed. *American Journal of Psychiatry*. doi:10.1176/appi.ajp.158.4.662
- Sharma, L., Kaur, J., & Shukla, G. (2012). Role of Oxidative Stress and Apoptosis in the Placental Pathology of *Plasmodium berghei* Infected Mice. *PLoS ONE*. doi:10.1371/journal.pone.0032694

- Singh, B., Kim Sung, L., Matusop, A., Radhakrishnan, A., Shamsul, S. S. G., Cox-Singh, J., ... Conway, D. J. (2004). A large focus of naturally acquired Plasmodium knowlesi infections in human beings. *Lancet*, *363*, 1017–1024. doi:10.1016/S0140-6736(04)15836-4
- Snow, R. W., Guerra, C. A., Noor, A. M., Myint, H. Y., & Hay, S. I. (2005). The global distribution of clinical episodes of Plasmodium falciparum malaria. *Nature*, *434*, 214–217. doi:10.1038/nature03342
- Telford, S. R. (1998). The development and persistence of phanerozoites in experimental infections of Plasmodium sasai. *International journal for parasitology*, *28*, 475–484. doi:10.1016/S0020-7519(97)00201-4
- Umbers, A. J., Aitken, E. H., & Rogerson, S. J. (2011). Malaria in pregnancy: small babies, big problem. *Trends in parasitology*, *27*, 168–175. doi:10.1016/j.pt.2011.01.007
- Vardo-Zalik, A. M., & Schall, J. J. (2009). Clonal diversity alters the infection dynamics of a malaria parasite (Plasmodium mexicanum) in its vertebrate host. *Ecology*, *90*, 529–536. doi:10.1890/07-1866.1
- Warrell, D. A., Looareesuwan, S., Phillips, R. E., White, N. J., Warrell, M. J., Chapel, H. M., ... Tharavanij, S. (1986). Function of the blood-cerebrospinal fluid barrier in human cerebral malaria: rejection of the permeability hypothesis. *The American journal of tropical medicine and hygiene*, *35*, 882–889.
- White, N. J., Pukrittayakamee, S., Hien, T. T., Faiz, M. A., Mokuolu, O. a, & Dondorp, A. M. (2013). Malaria. *Lancet*, *6736*, 1–13. doi:10.1016/S0140-6736(13)60024-0

Wiersch, S. C., Maier, W. A., & Kampen, H. (2005). Plasmodium (Haemamoeba) cathemerium gene sequences for phylogenetic analysis of malaria parasites. *Parasitology research*, *96*, 90–94.
doi:10.1007/s00436-005-1324-8

Tables

Table 1. The Rapid murine Coma and Behavior Scale (RMCBS).

Label	Score	Description
Coordination		
Gait	(0-2)	(none – ataxic – normal)
Balance	(0-2)	(no body extension – extended feet on wall – entire body lift)
Exploratory Behavior		
Motor Performance	(0-2)	(none – 2-3 corners explored in 90 seconds – explores 4 corners in 15 seconds)
Strength and Tone		
Body Position	(0-2)	(on side – hunched – full extension)
Limb Strength	(0-2)	(hypotonic, no grasp – weak pull-back – strong pull-back)
Reflexes and Self-Preservation		
Touch Escape	(0-2)	(none – unilateral – instant and bilateral; in 3 attempts)
Pinna Reflex	(0-2)	(none – unilateral – instant and bilateral; in 3 attempts)
Toe Pinch	(0-2)	(none – unilateral – instant and bilateral; in 3 attempts)
Aggression	(0-2)	(none – bite attempt with tail cut – bite attempt prior to tail cut, in 5 seconds)
Hygiene-Related Behavior		
Grooming	(0-2)	(ruffled, with swaths of hair out of place – dusty/piloerection – normal/clean with sheen)

The RMCBS consists of 10 parameters, and each parameter is scored 0 to 2, with a 0 score correlating with the lowest function and a 2 score, that highest. An animal can achieve an accumulative score of 0 to 20.

Table 2. Pregnancy outcome obtained caesarean section on G18 after *P. berghei* infection during pregnancy.

	Number of fetus	Mortality rate (%)	Number of resorption	Number of premature	weight of fetus (g)	weight of placenta (g)
Infected	7±0.58	100±0	2.33±0.33	1±1	0.69±0.070	0.114±0.026
Uninfected	9.33±1.20	0±0	0.33±0.33	0±0	0.78±0.093	0.083±0.012

All values are means ± SD.

Figure legends

Figure 1. *Plasmodium* parasites and their vertebrate hosts. *Plasmodium* parasites infect human and other animals, including monkeys, birds, reptiles and rodents.

Figure 2. Classical pathological features of human malaria. The clinical features of human malaria cover a spectrum from mild case such as parasitemia, fever, anemia and splenomegaly to severe cases leading to death. Severe malaria has manifestations cerebral malaria and respiratory distress etc.

Figure 3. Increase of pRBCs during infection with 10^6 *P. berghei* in C57BL/6 and BALB/c. The time course of parasitemia (%) in *P. berghei*-infected C57BL/6 (A) and BALB/c (B). Parasitemia levels were measured on Giemsa-stained blood smears on dpi 0, 2, 4 and 6. Means and SD are shown.

Figure 4. Decrease of the hematocrit level during infection with *P. berghei*. The time course of the hematocrit level in *P. berghei*-infected C57BL/6 (A) and BALB/c (B). The hematocrit levels were measured on dpi 0, 2, 4 and 6. Means and SD are shown. * $P < 0.01$.

Figure 5. Concentrations of serum components in *P.berghei*-infected mice.

The concentrations of TP, ALB, BUN, CRE, Na, K, Cl, Ca, IP, Fe, AST, ALT, LDH, AMY, γ -GT, T-CHO, TG, HDL-C, GLU and T-BIL in the serum of infected were measured by blood biochemical examination on dpi6. Means and SD are shown. * $P < 0.01$. Naive C57BL/6: C n, infected C57BL/6: C i, naive BALB/c: B n, infected BALB/c: B i. TP: total protein, ALB: albumin, BUN: blood urea nitrogen, CRE: creatinine, Na: natrium, K: kalium, Cl: chlore, Ca: calcium, IP: inorganic phosphorus, Fe: iron, AST: aspartate aminotransferase, ALT: alanine aminotransferase, LDH: lactase dehydrogenase, AMY: amylase, γ -GT: γ -glutamyltransferase, T-CHO: total cholesterol, TG: triglyceride, HDL-C: high-density lipoprotein, GLU: glucose T-BIL: total bilirubin.

Figure 6. Weight loss in *P. berghei*-infected C57BL/6. The time course of weight (g) in *P. berghei*-infected C57BL/6 (A) and BALB/c (B). Mice were weighted on dpi 0, 2, 4 and 6. Means and SD are shown. * $P < 0.01$.

Figure 7. Piloerection of *P. berghei*-infected Mice. The pictures of *P. berghei*-infected C57BL/6 (A), BALB/c (B) on dpi 6 and naive C57BL/6 (C), BALB/c (D) were indicated.

Figure 8. Decrease of RMCBS scores in *P. berghei*-infected C57BL/6. The time course of RMCBS scores in *P. berghei*-infected C57BL/6 (A) and BALB/c (B) were indicated. RMCBS tests were performed on dpi 0, 2, 4 and 6. Means and SD are shown. * $P < 0.01$.

Figure 9. Decrease of the number of breaths per minute in *P. berghei*-infected C57BL/6. The time course of the number of breaths per minute in *P. berghei*-infected C57BL/6 (A) and BALB/c (B). The number of breaths per minute was measured on dpi 0, 2, 4 and 6. Means and SD are shown. * $P < 0.01$.

Figure 10. Splenomegaly in mice infected with *P. berghei*. *Panel A:* The pictures of *P. berghei*-infected and naive spleens. *Panel B:* Weight of the spleen was compared between naive or infected mice. Means and SD in each group are shown. * $P < 0.01$.

Figure 11. Color alternation of organs and red spots on the skin in C57BL/6. *Panel A:* The pictures of *P. berghei*-infected and naive brains. *Panel B:* The pictures of *P. berghei*-infected and naive lungs. *Panel C:* The pictures of *P. berghei*-infected and naive livers with gallbladders. *Panel D:* The pictures of *P. berghei*-infected and naive kidneys with adrenal glands. *Panel E:* The pictures of *P. berghei*-infected and naive skins.

Figure 12. The conclusion of chapter 1. Parasitemia, Anemia, splenomegaly, liver and gallbladder injury occurred in both strains. On the other hand, consciousness and movement disturbance, respiration failure and abnormal bleeding occurred only in *P. berghei*-infected C57BL/6. These results indicated that *P. berghei*-infected C57BL/6 had several severe manifestations that weren't occurred in BALB/c even though rate of infection was same.

Figure 13. The image of mice brain and its blood-brain barrier. Picture of whole brain of mice and image of BBB were shown.

Figure 14. Increase of pRBCs during infection with 10^6 *P. berghei* in C57BL/6. The time course of parasitemia (%) in *P. berghei*-infected C57BL/6. Parasitemia levels were measured on Giemsa-stained blood smears every day. Means and SD are shown.

Figure 15. Exudation of Evans blue to cerebral parenchyma. The pictures of whole and frontal section of brains in infected C57BL/6 (A) and naive C57BL/6 (B) after Evans blue injection.

Figure 16. No leakage of hemocytes to cerebral parenchyma. HE stained sections of capillary of cerebrum in infected C57BL/6 on dpi 6 (A) naive

C57BL/6 (B) are depicted. Scale bars indicated 10 μm . Arrows indicated malaria pigment.

Figure 17. Exudation of IgG to cerebral parenchyma. Localization of IgG was examined by immunohistochemical analysis in infected C57BL/6 on dpi 6 (A) and naive C57BL/6 (B). Scale bars indicated 50 μm .

Figure 18. Hypothetical schema of breakdown of BBB in the development of the consciousness disturbance. After *P. berghei*-infection, vessel hyperpermeability and breakdown of BBB were occurred. Following these phenomena, cerebral edema was formed and causes the consciousness disturbance.

Figure 19. The images of mice lung and image of its alveoli.

Picture of whole lung of mice and image of alveoli were shown.

Figure 20. Increase of pRBCs during infection with 10^6 *P. berghei* in C57BL/6. The time course of parasitemia (%) in *P. berghei*-infected C57BL/6. Parasitemia levels were measured on Giemsa-stained blood smears every day. Means and SD are shown.

Figure 21. RBCs accumulation in alveolar capillaries and fluid accumulation

in alveolar space. HE stained sections of lung in infected C57BL/6 on dpi6 (A,B,D,E) and naive C57BL/6 (C,F) are depicted. Scale bars indicated 20 μm (A-C) and 5 μm (D-F). Arrows indicated malaria pigment.

Figure 22. Exudation of Evans blue from the vessels of lung in infected C57BL/6. The pictures of lungs in infected C57BL/6 (A) and naive C57BL/6 (B) after Evans blue injection.

Figure 23. Hypothetical schema of vessel hyperpermeability in the development of the respiration failure. After *P. berghei* infection, vessel hyperpermeability was occurred in the alveoli. Following these phenomena, pulmonary edema was formed and causes the respiration failure.

Figure 24. The images of mice placenta and image of its placental barrier on G18. Images of mice placenta and placental barrier on gestation day 18 were shown.

Figure 25. Decrease survival rate and weight of newborns from infected mother. Mortality rate of newborns from 10^7 , 10^6 , 10^5 *P. berghei*-infected mothers and naive mothers (A). Means are shown. Weight of newborns from 10^7 , 10^6 , 10^5 *P. berghei*-infected mothers and naive mothers (B). Means and

SD in each group are shown. * $P < 0.01$. The pictures of the newborn from 10^7 infected *P. berghei*-infected mother (C) and the newborn from naive mother (D). Scale bar indicated 1 cm.

Figure 26. Increase of pRBCs and decrease maternal weight in 10^7 pRBCs-infected mothers. The time course of parasitemia (%) in 10^7 *P. berghei*-infected pregnant and non-pregnant (A). Parasitemia levels were measured on Giemsa-stained blood smears every day. The time course of maternal weight in 10^7 *P. berghei*-infected pregnant and non-pregnant (B). Means and SD in each group are shown. * $P < 0.01$.

Figure 27. Pregnancy outcome of 10^7 pRBCs-infected mothers. The pictures of uterus in infected (A) and naive (B) on G18. The pictures of fetus with placenta in infected (C) and naive (D) on G18. Arrows indicated resorption.

Figure 28. Penetration of junctional zone in placenta from infected mother. HE stained sections of placenta in infected (A) and naive (B) are depicted. Dot-lines were put around the junctional zone. Scale bars indicated 1 mm.

Figure 29. RBCs accumulation and abnormally proliferation of spongiotrophoblast cells in the junctional zone. HE stained sections of placenta on G18 in infected and naive are depicted. Scale bars indicated 50,

20 and 5 μm .

Figure 30. Decrease of cytotrophoblast cells in labyrinth zone. HE stained sections of placenta on G18 in infected (A) and naive (B) are depicted. Scale bars indicated 20 μm . Arrows indicated cytotrophoblast cell.

Figure 31. Destruction of syncytiotrophoblast cells in labyrinth zone. Localization of syncytin, expressing in only syncytiotrophoblast cells was examined by immunohistochemical analysis in infected (A) and naive (B) on G18. Scale bars indicated 20 μm .

Figure 32. Hypothetical schema of breakdown of placental barrier in the development of stillbirth. After maternal *P. berghei* infection, the destruction of placental barrier occurred. Following this phenomenon, change of placental barrier permeability occurred and causes the stillbirth.

Figure 33. General hypothetical schema of the change of vessel permeability in the development of severe manifestations in *P. berghei*-infected C57BL/6. *P. berghei*-infected C57BL/6 has several severe manifestations and the change of vessel permeability plays a part of pathogenesis of them in common.

Figures

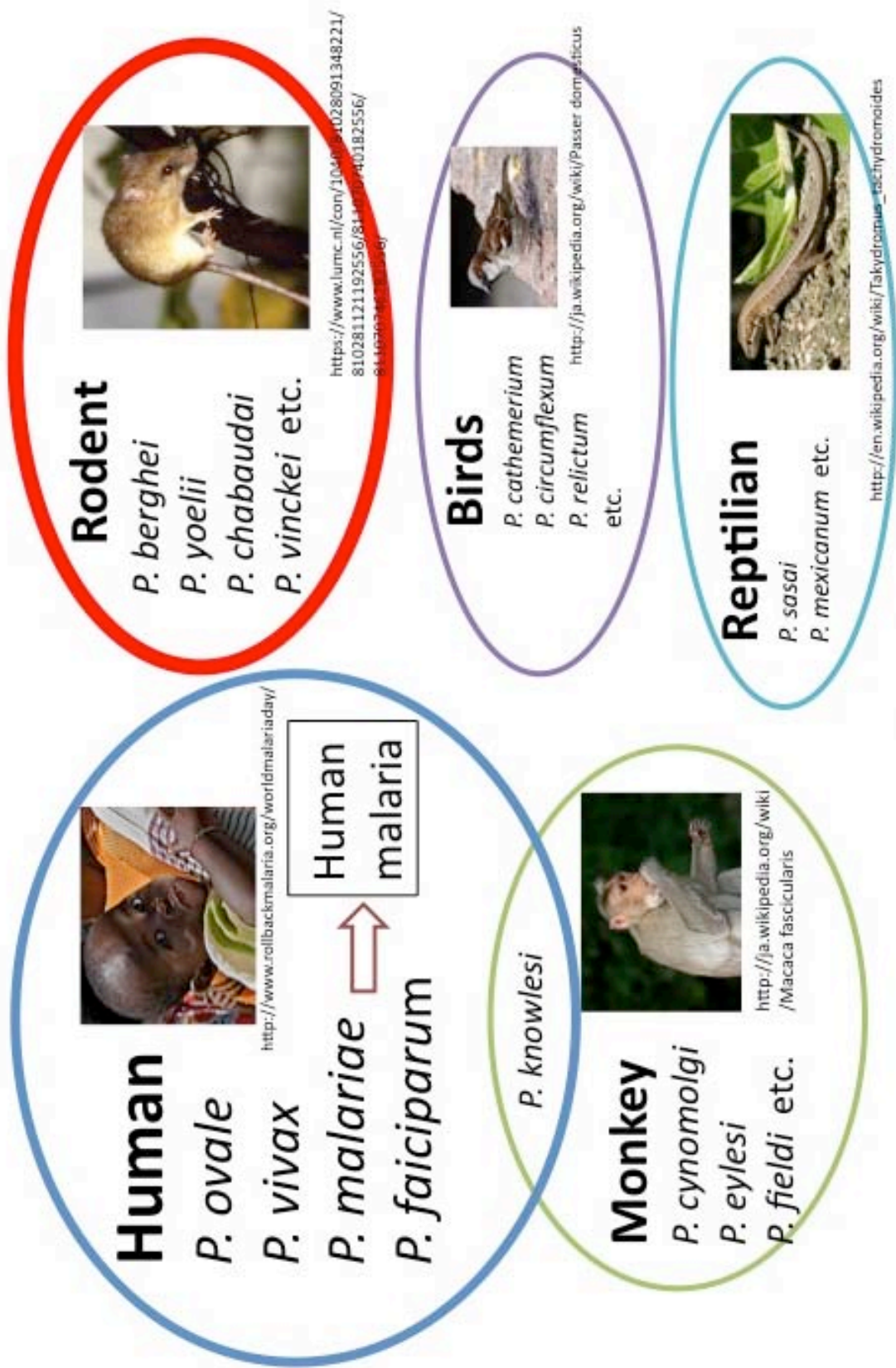


Fig. 1

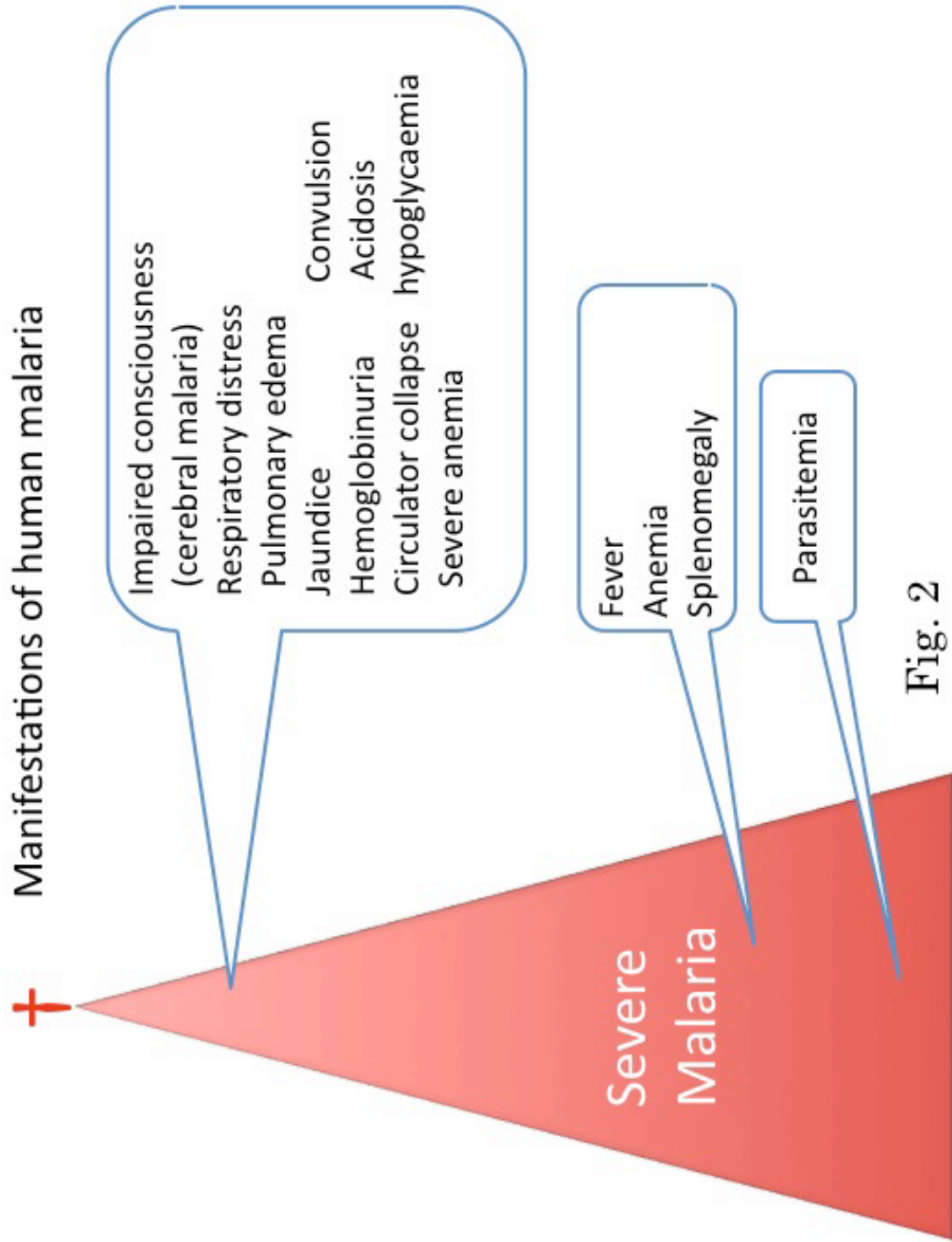
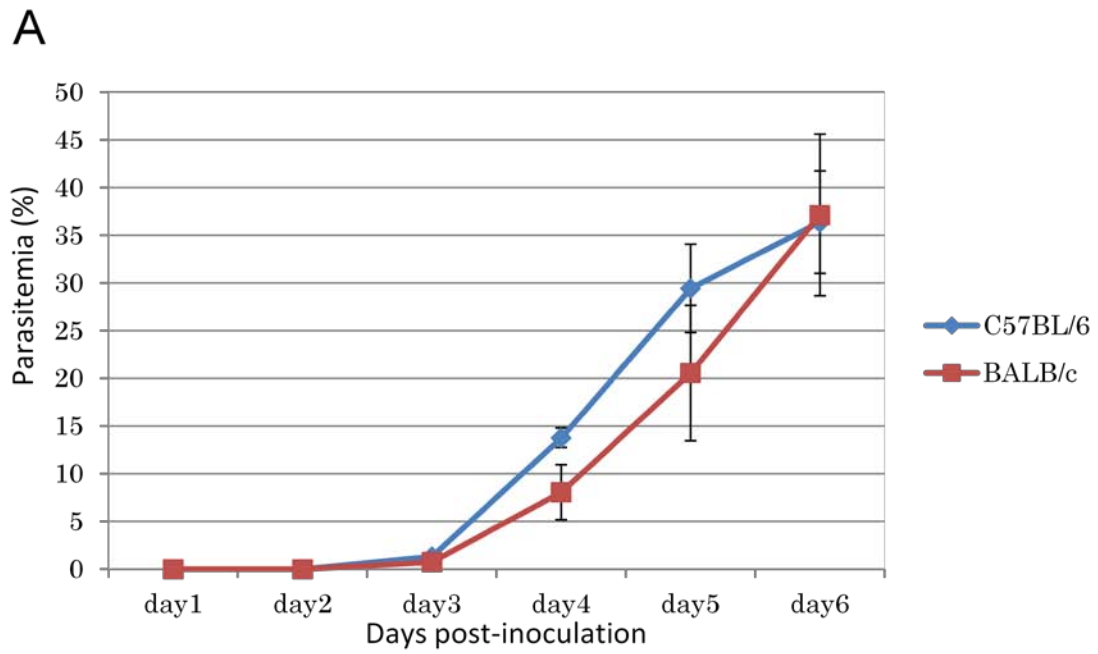


Fig. 2



B **C57BL/6** **BALB/c**

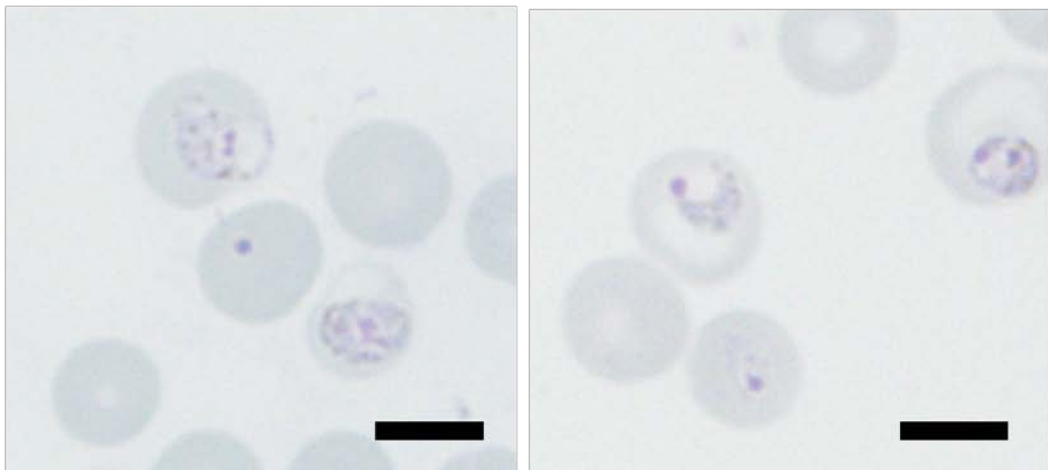


Fig. 3

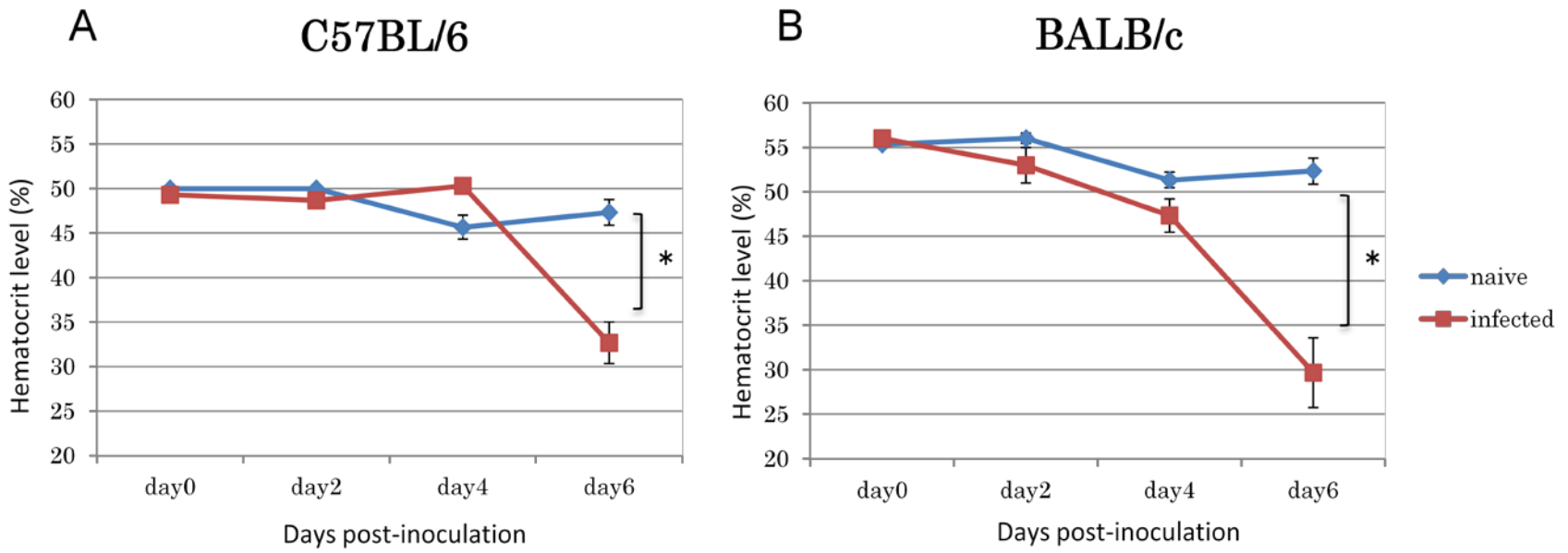


Fig. 4

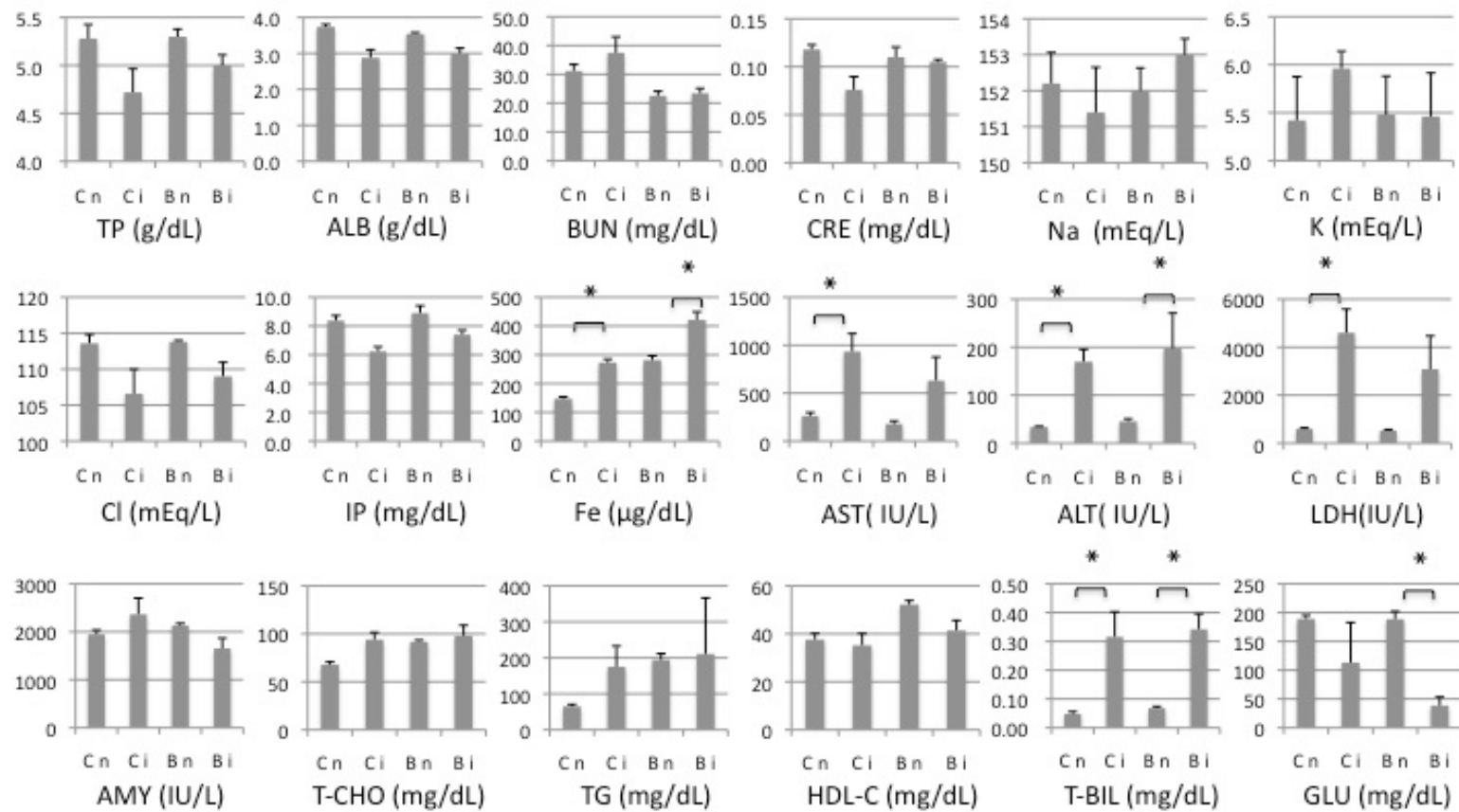


Fig. 5

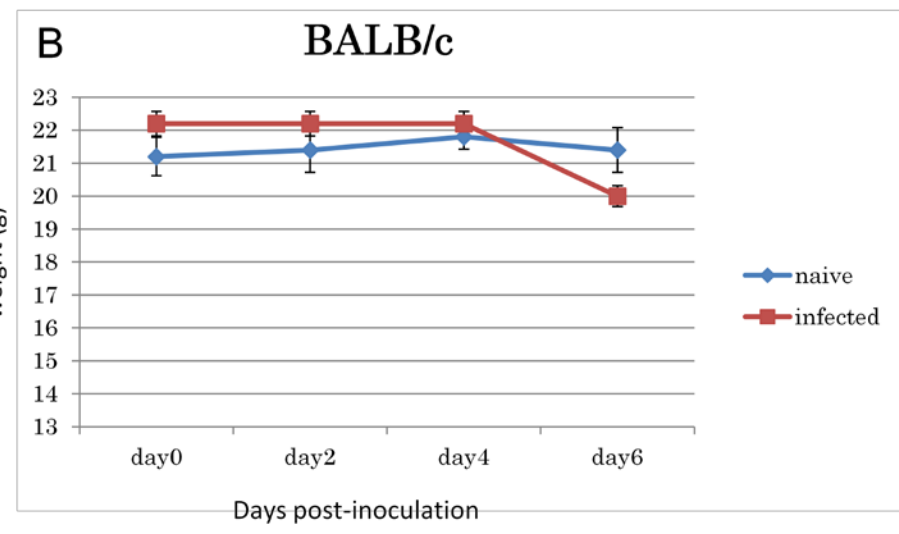
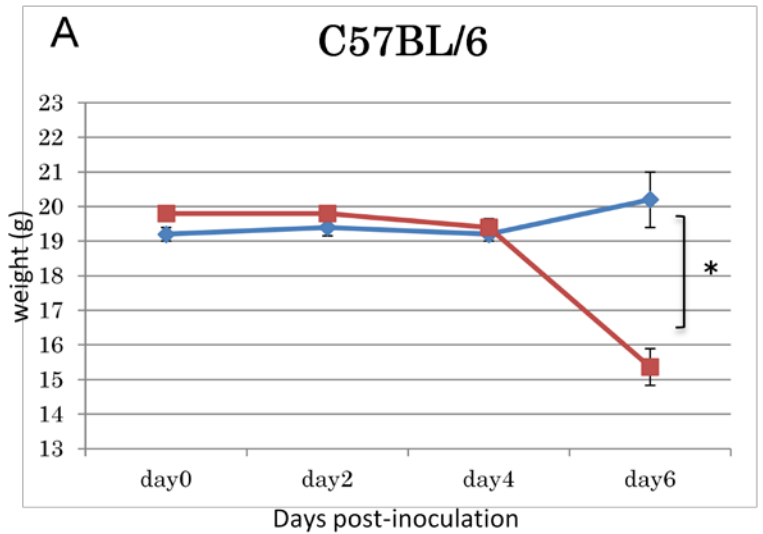


Fig. 6

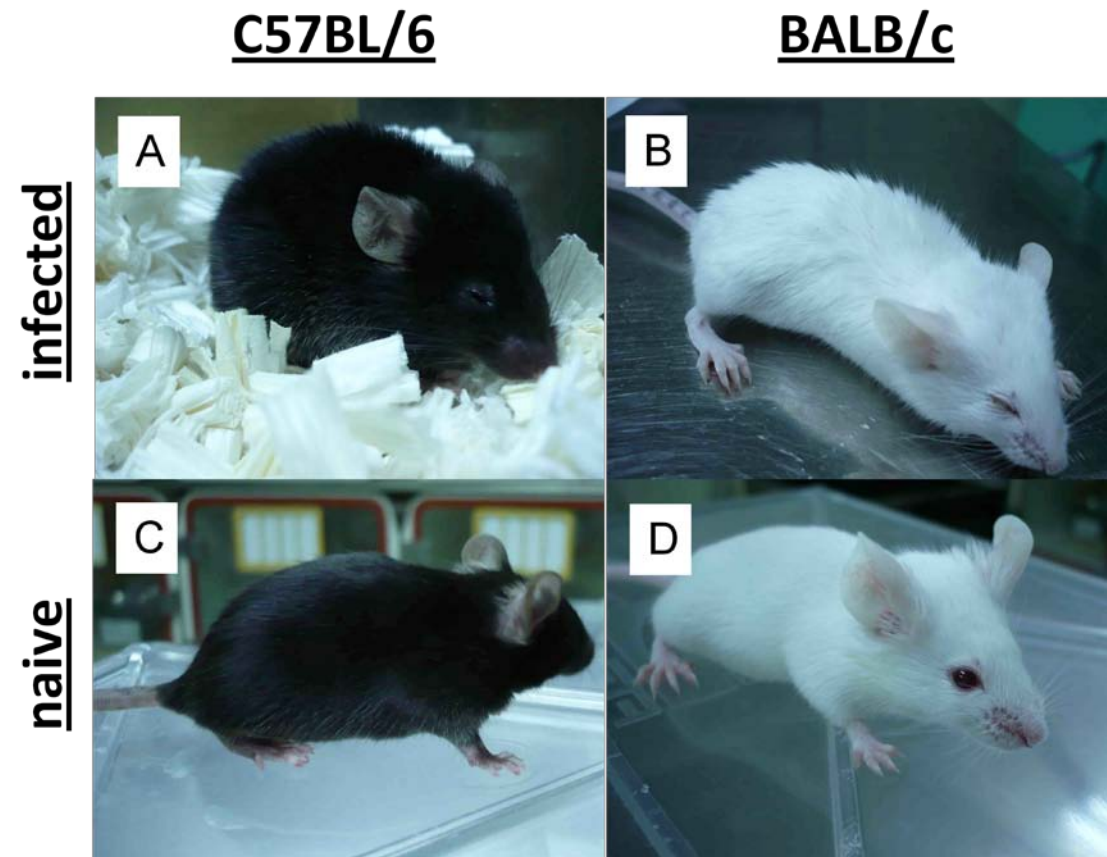


Fig. 7

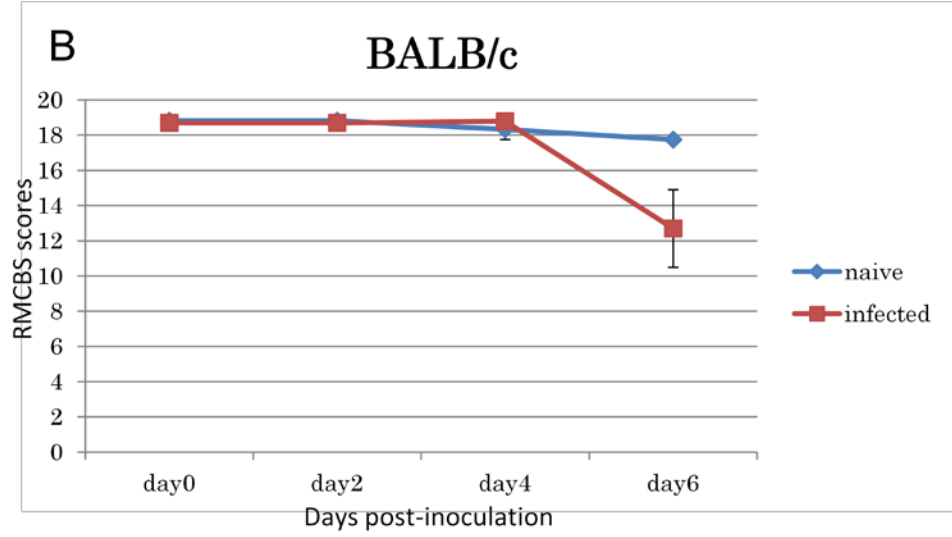
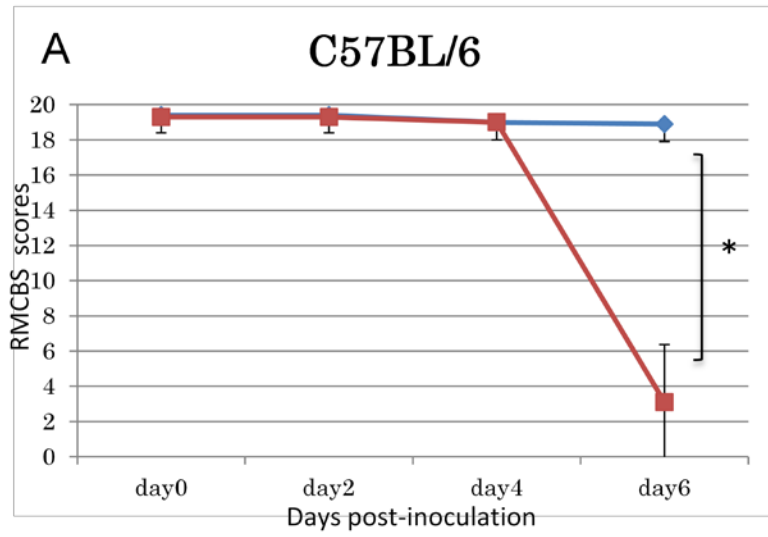


Fig. 8

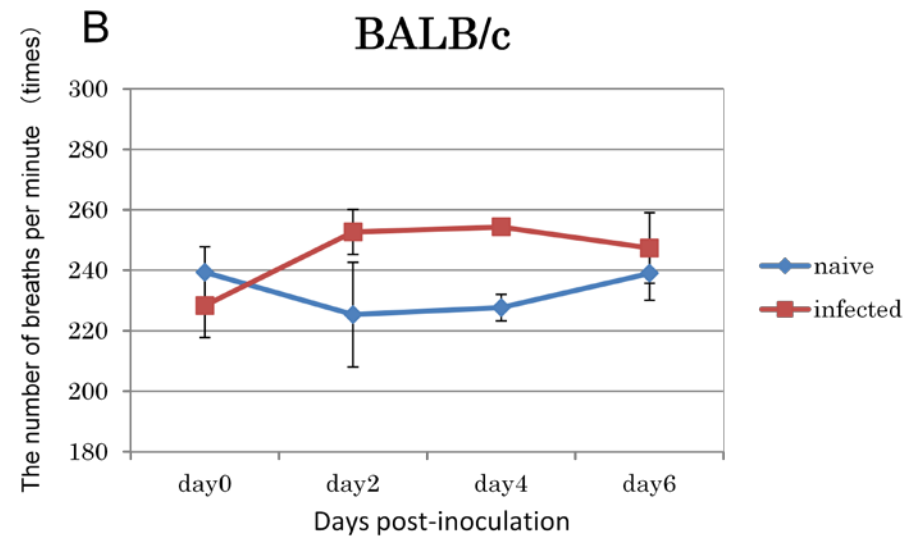
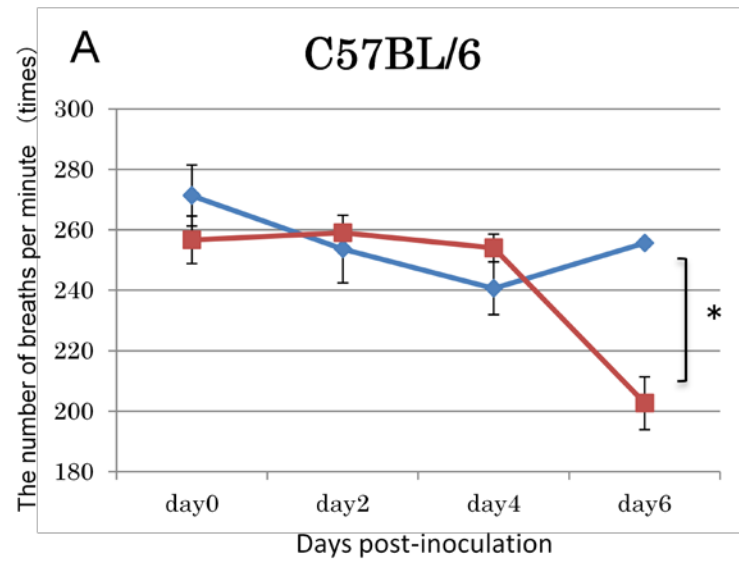


Fig. 9

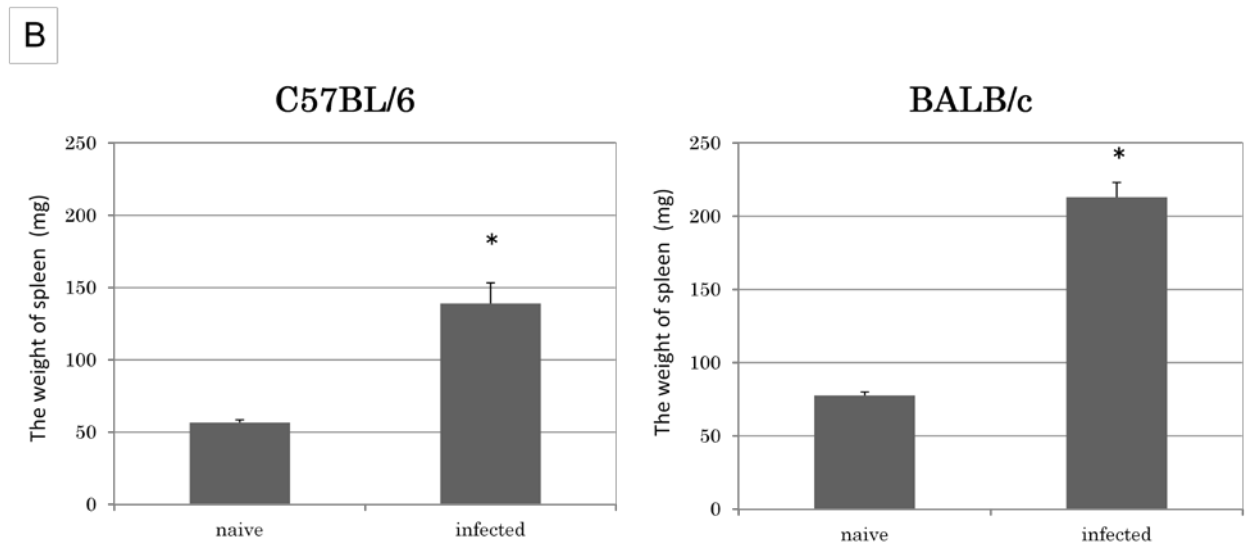


Fig. 10

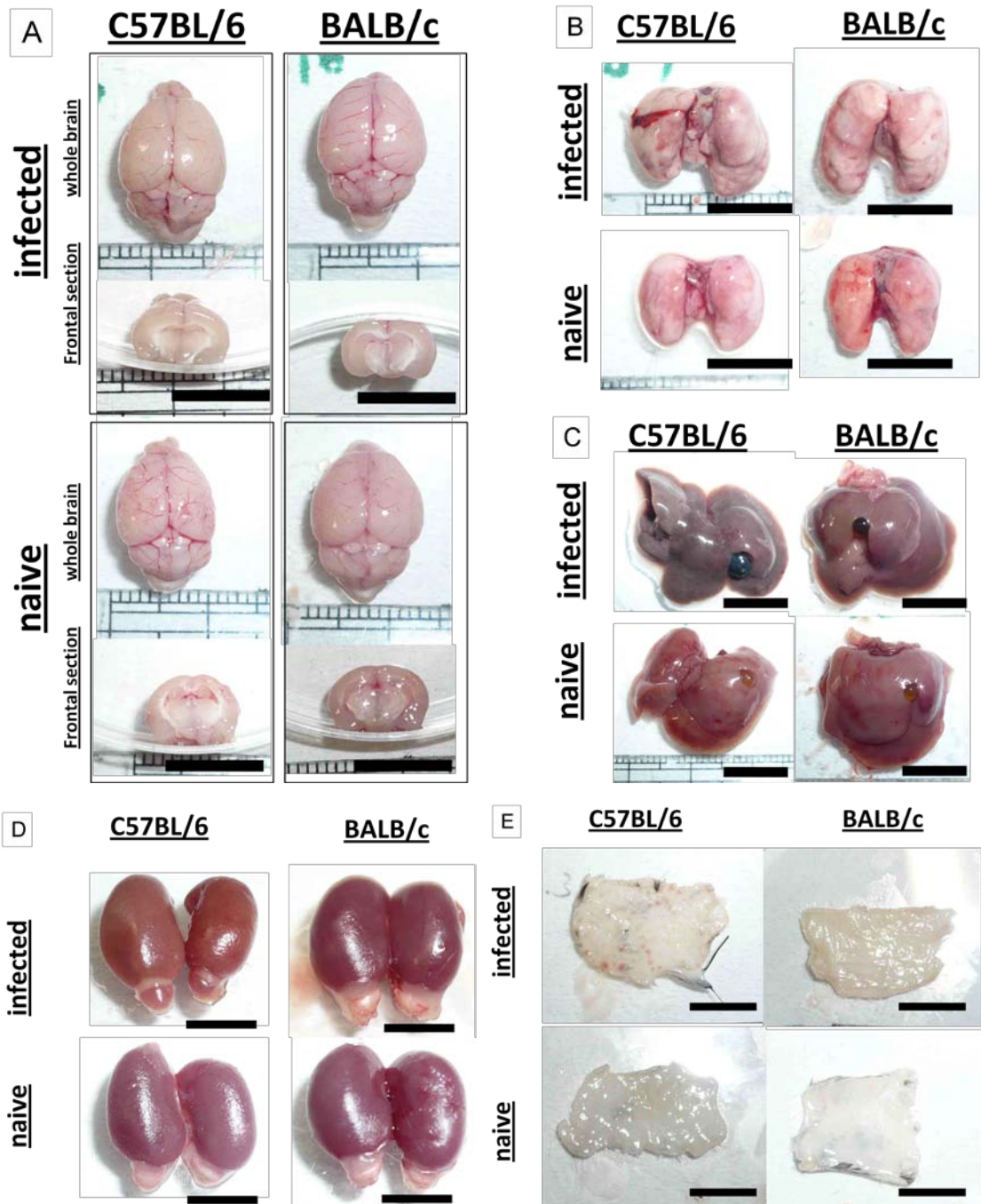


Fig. 11

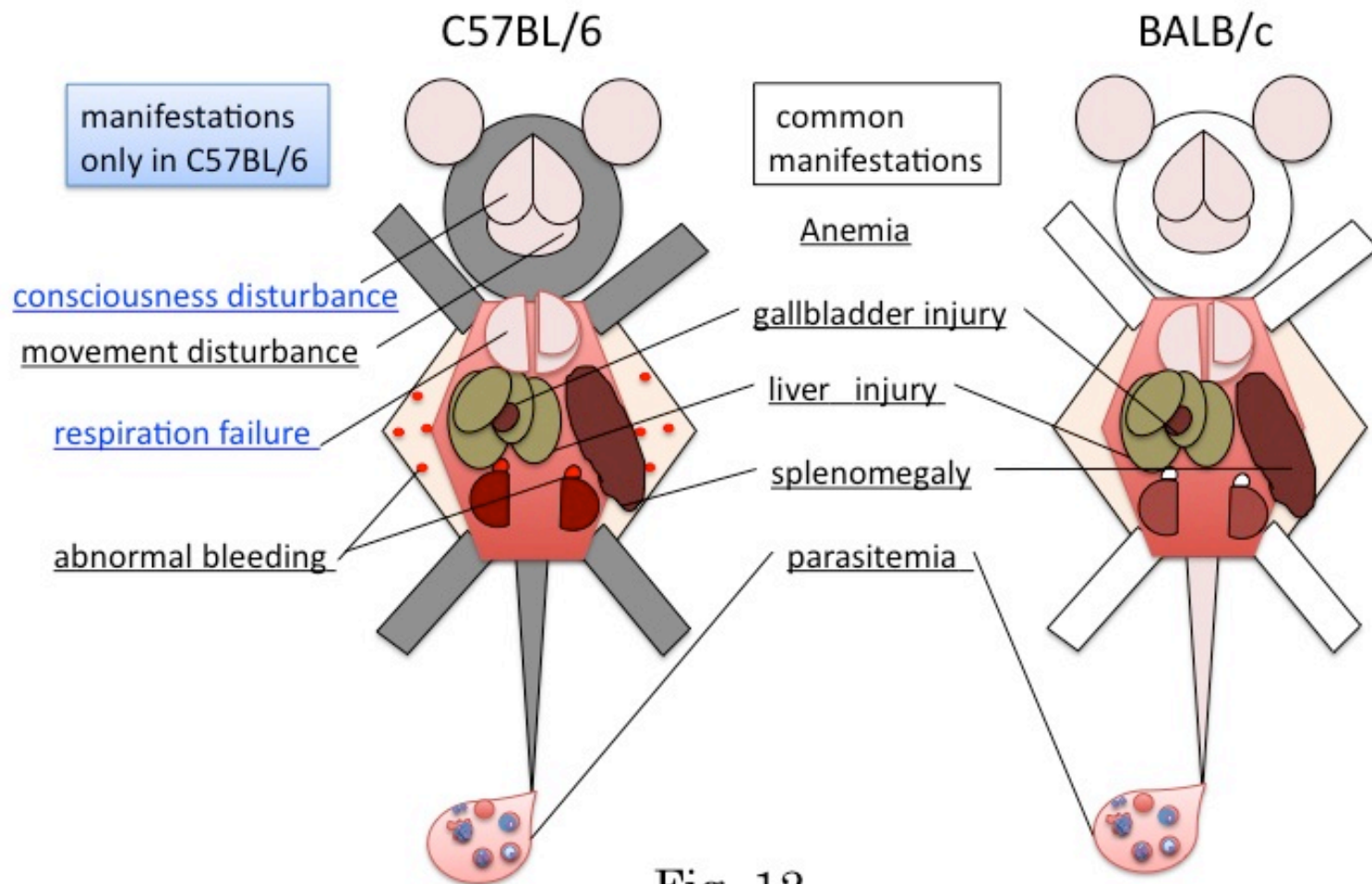


Fig. 12

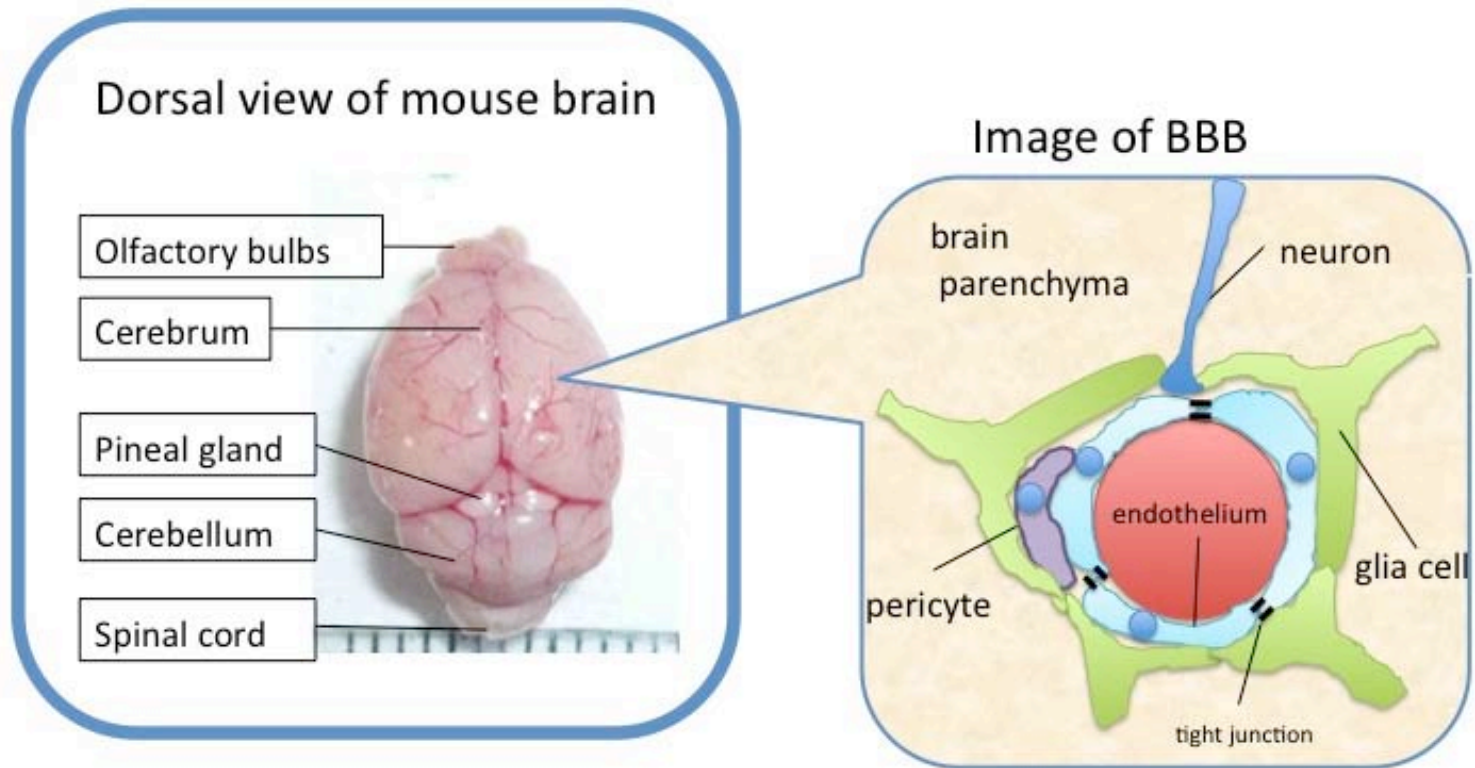


Fig. 13

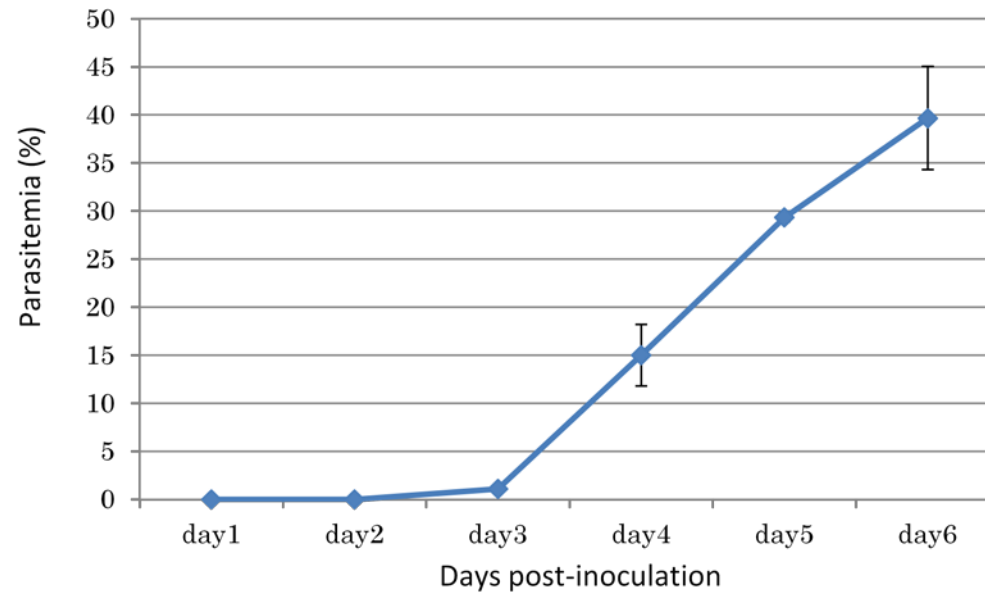


Fig. 14

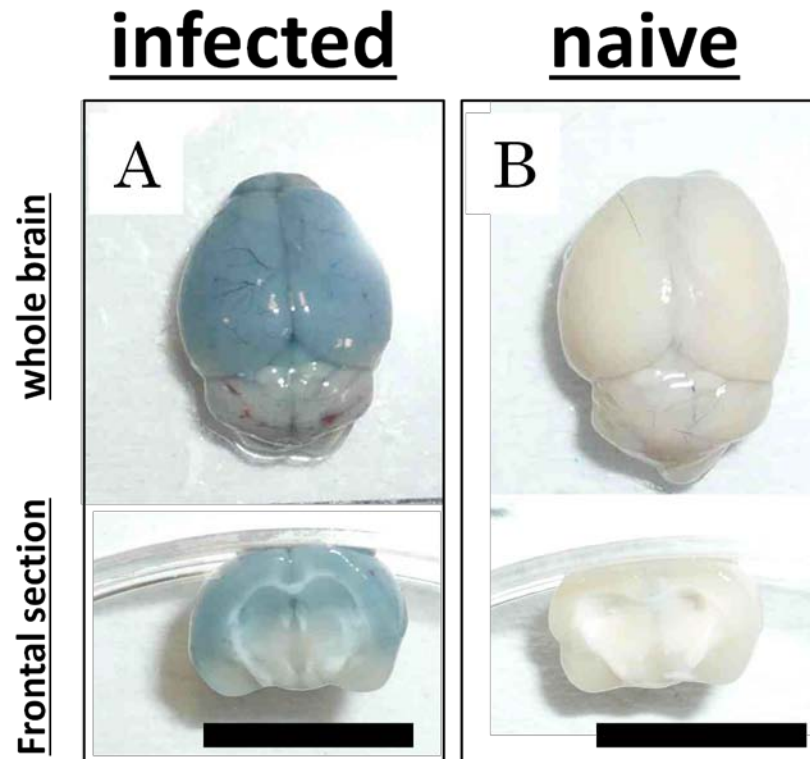
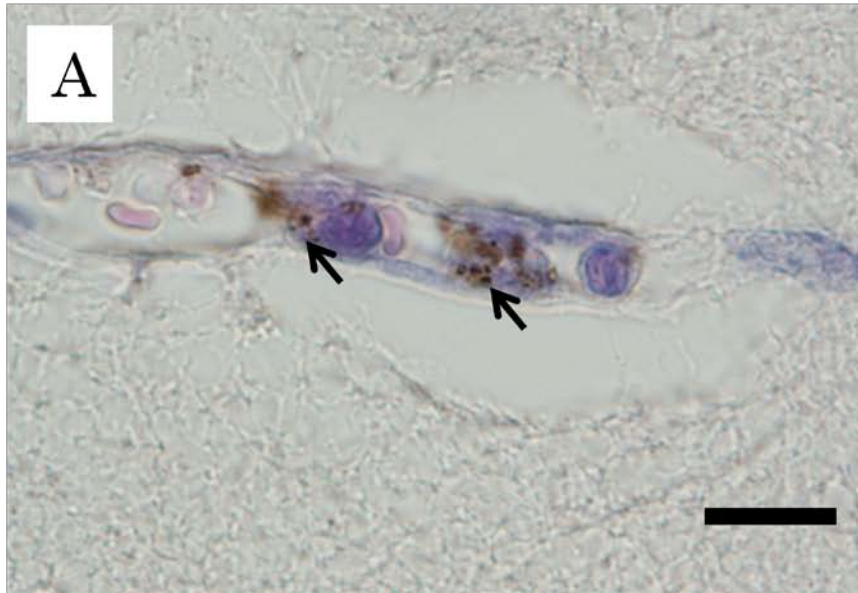


Fig. 15

infected



naive



Fig. 16

infected

naive

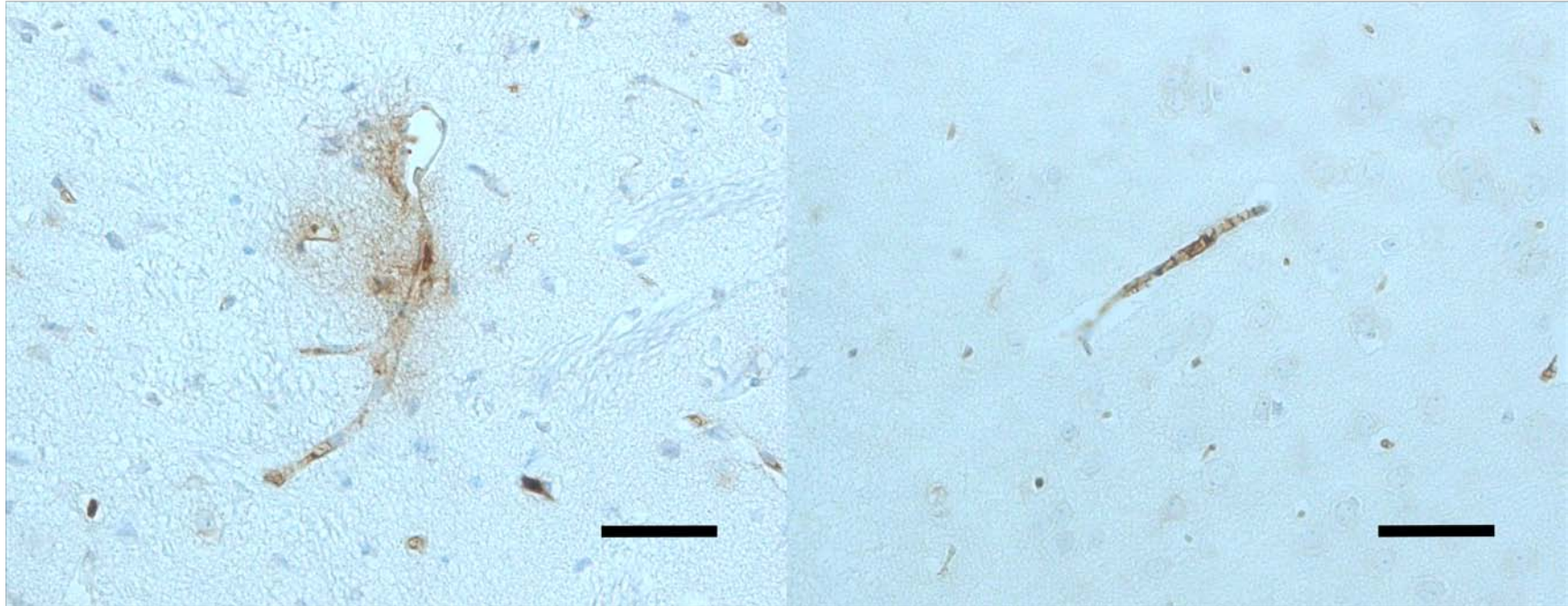


Fig. 17

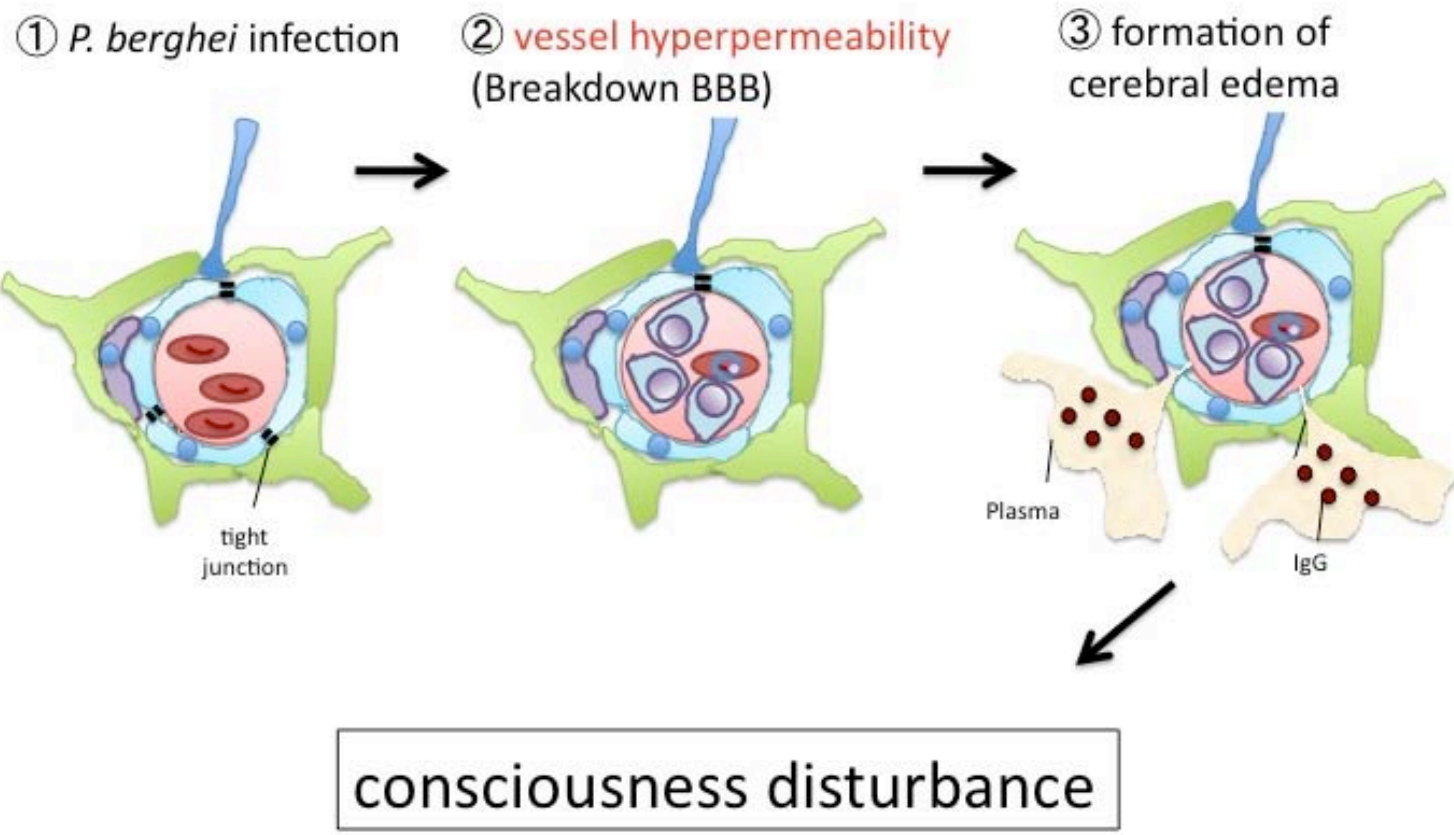


Fig. 18

Mouse lung



Image of alveoli

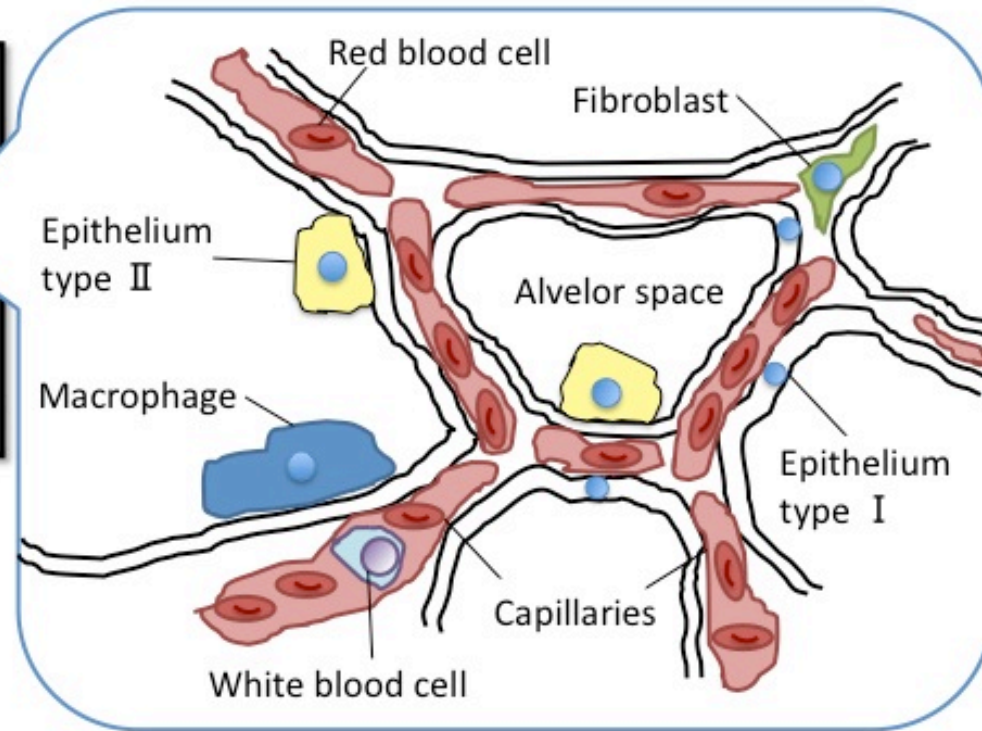


Fig. 19

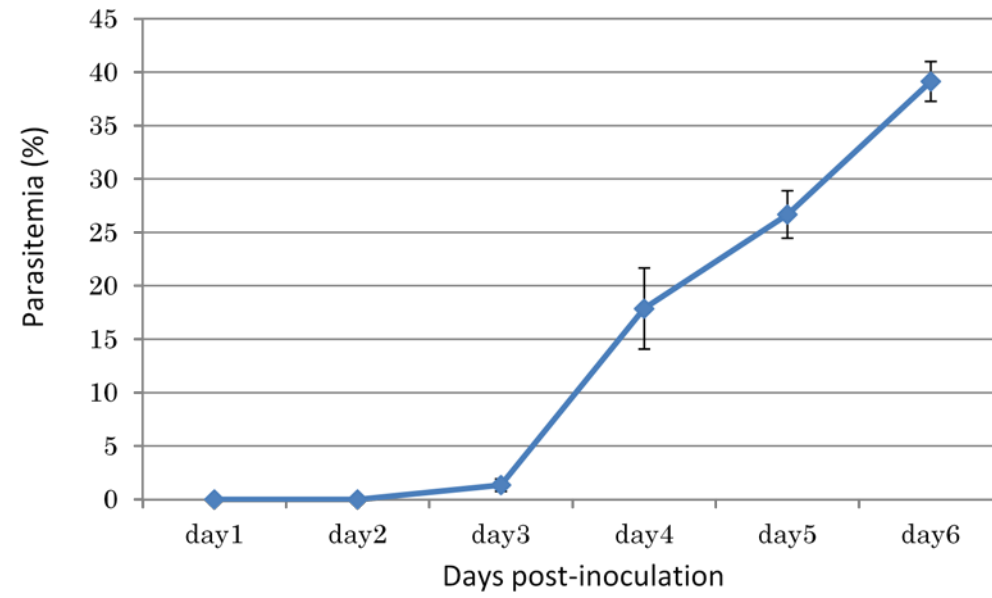


Fig. 20

infected

naive

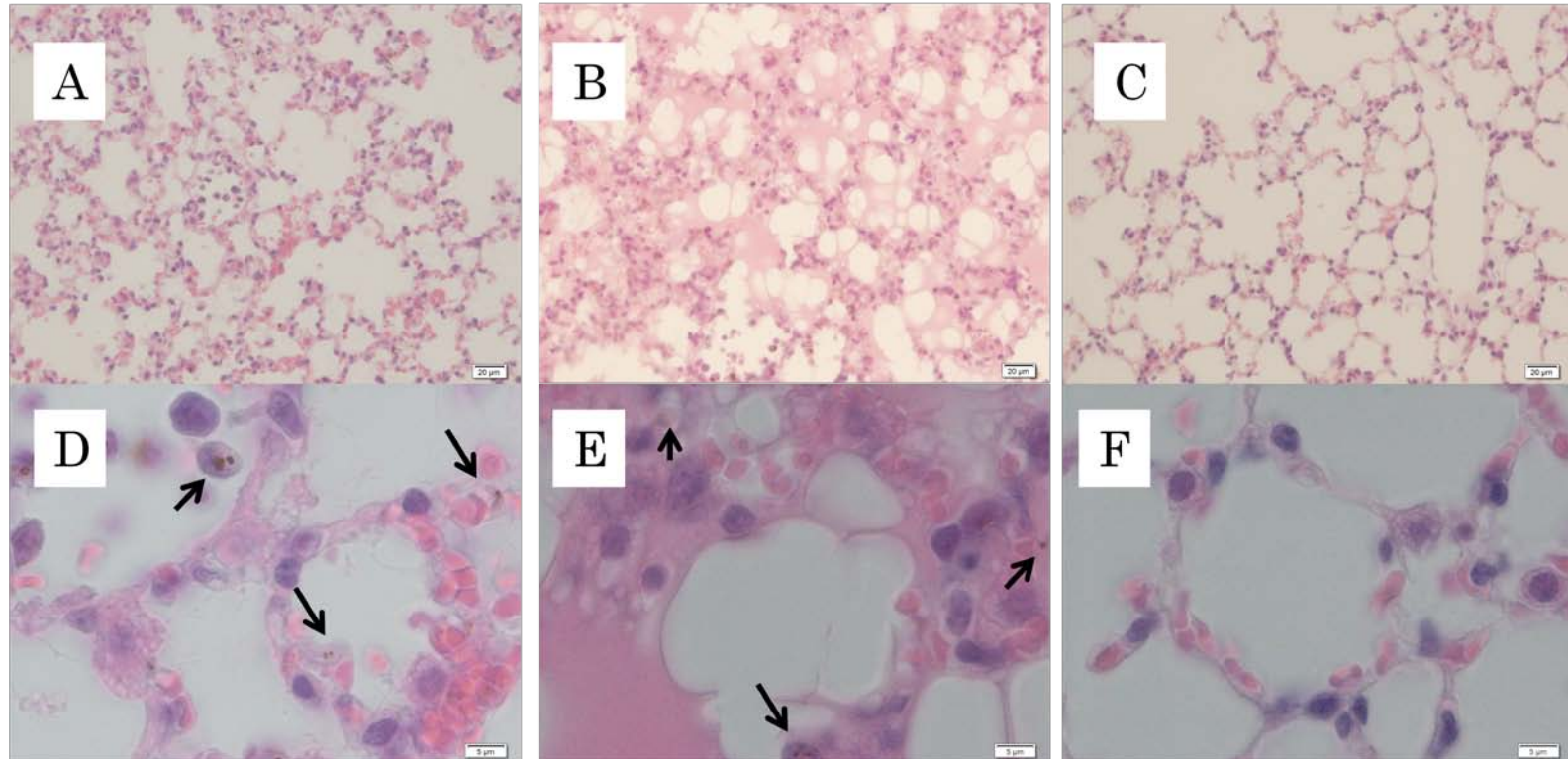


Fig. 21

infected

naive



Fig. 22

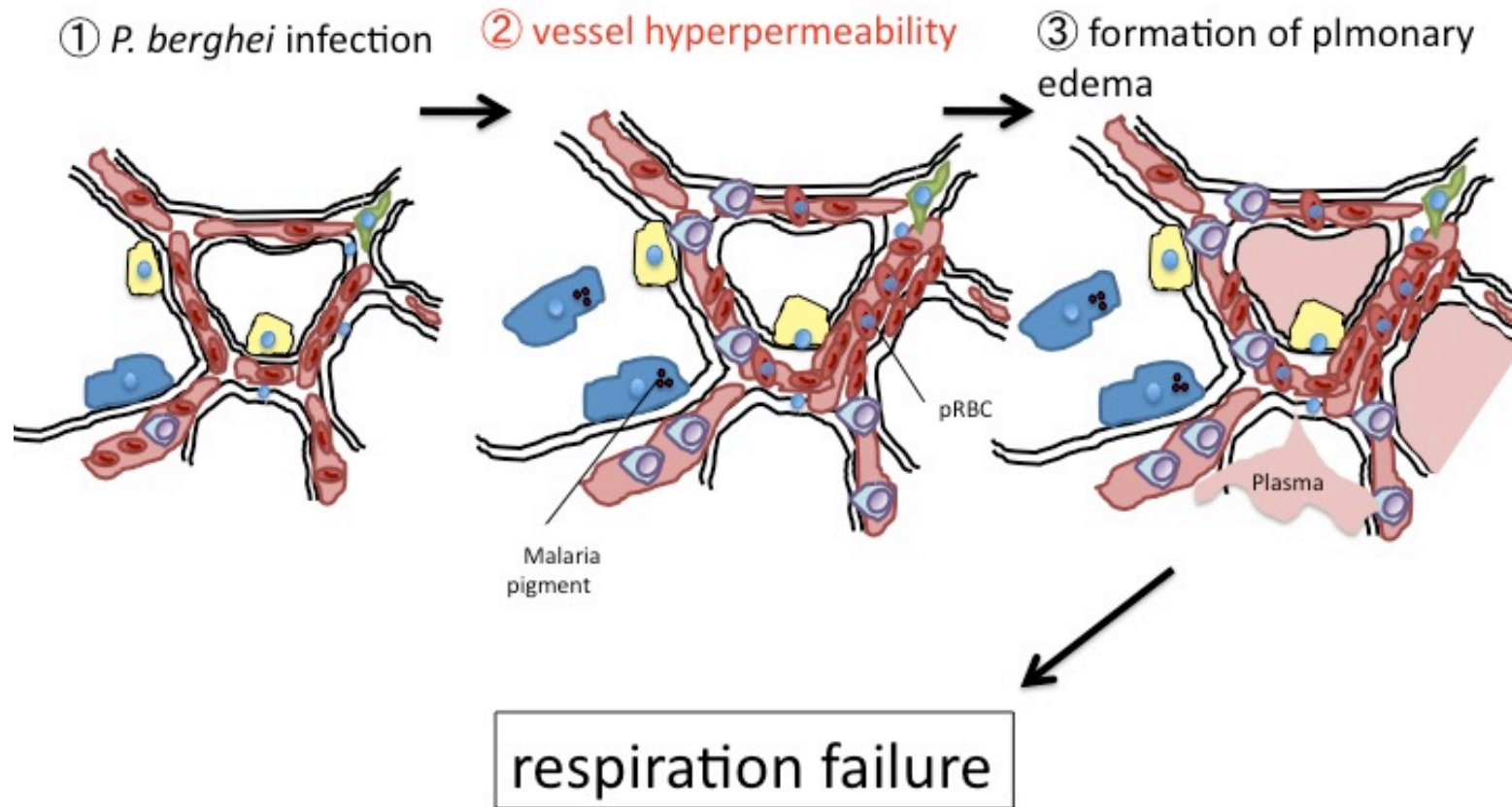


Fig. 23

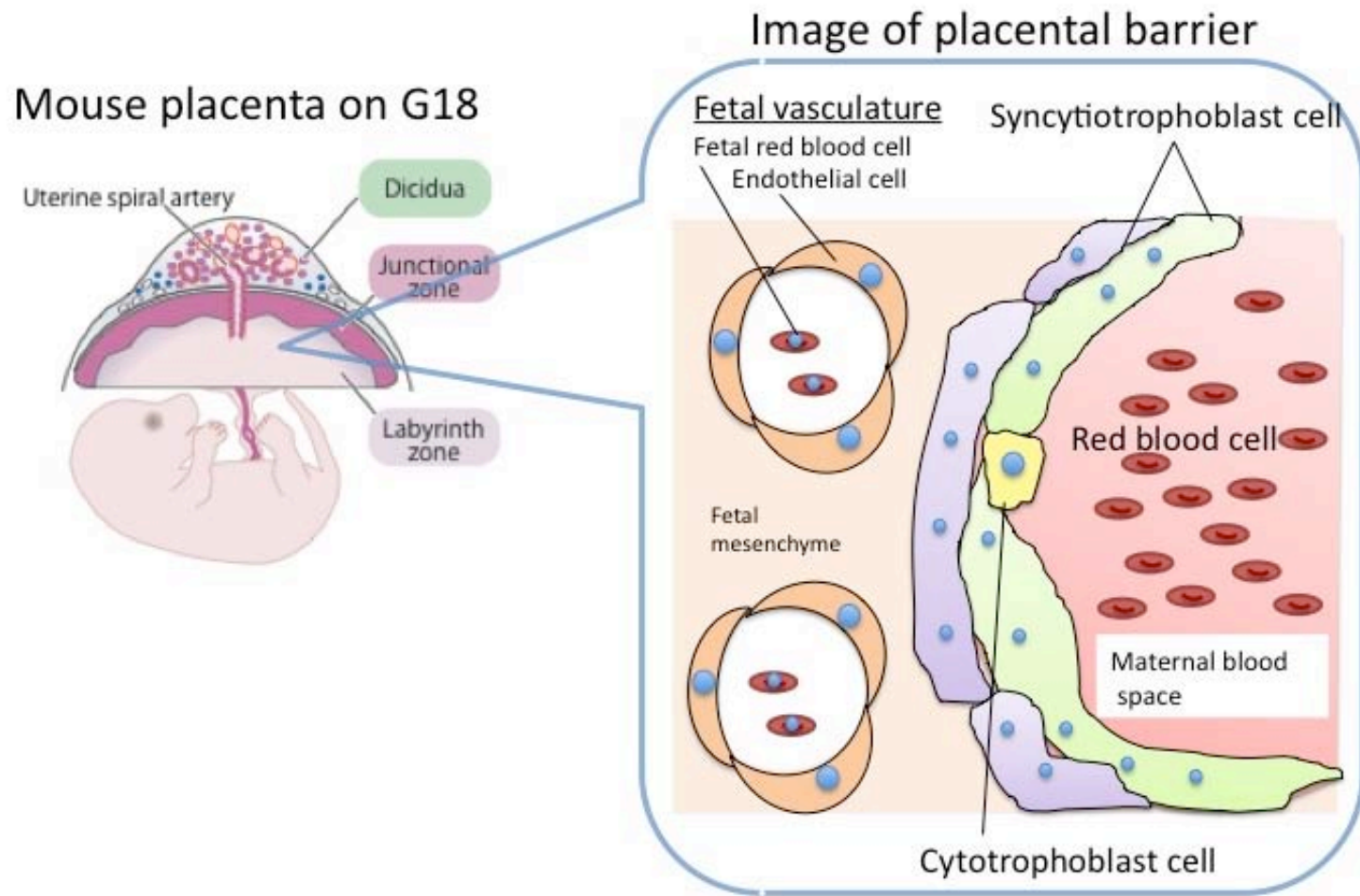


Fig. 24

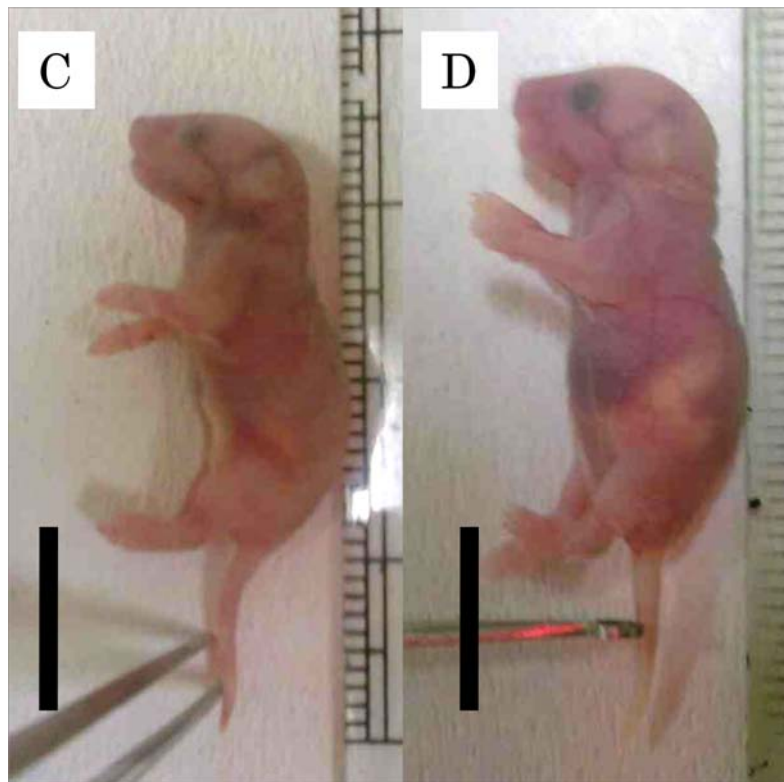
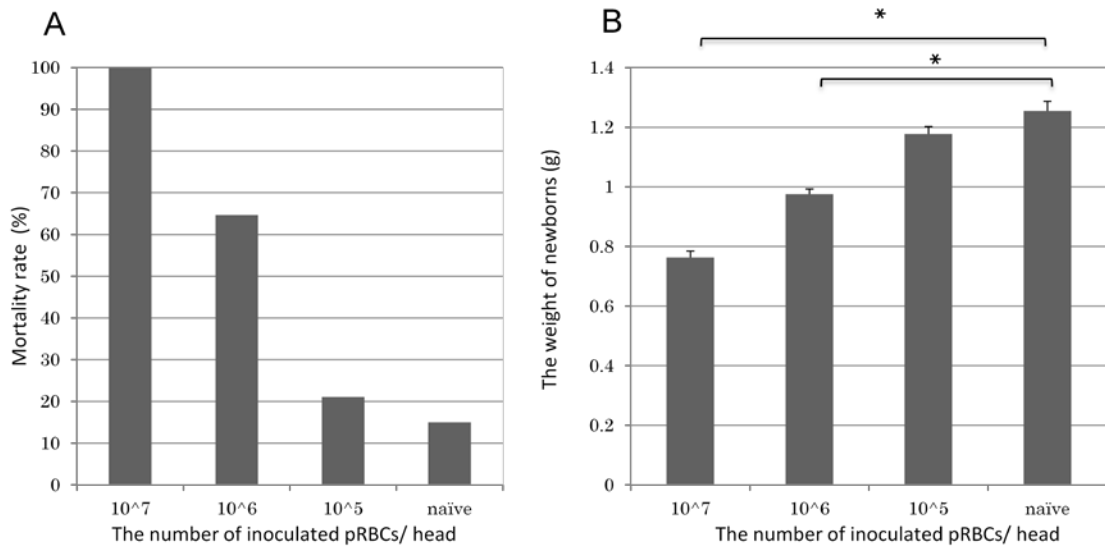


Fig. 25

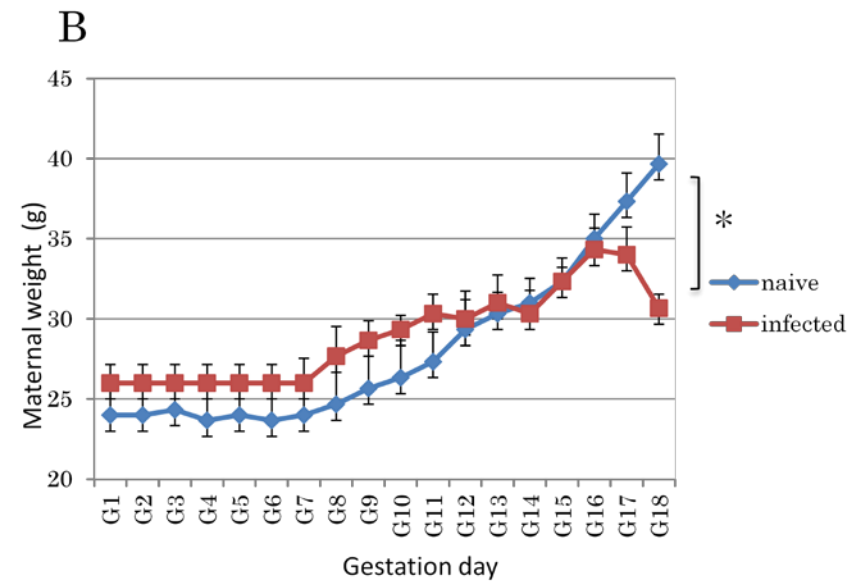
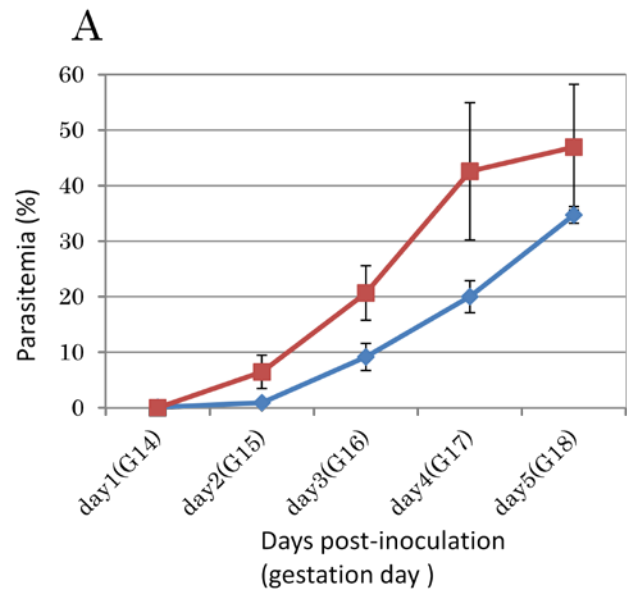


Fig. 26

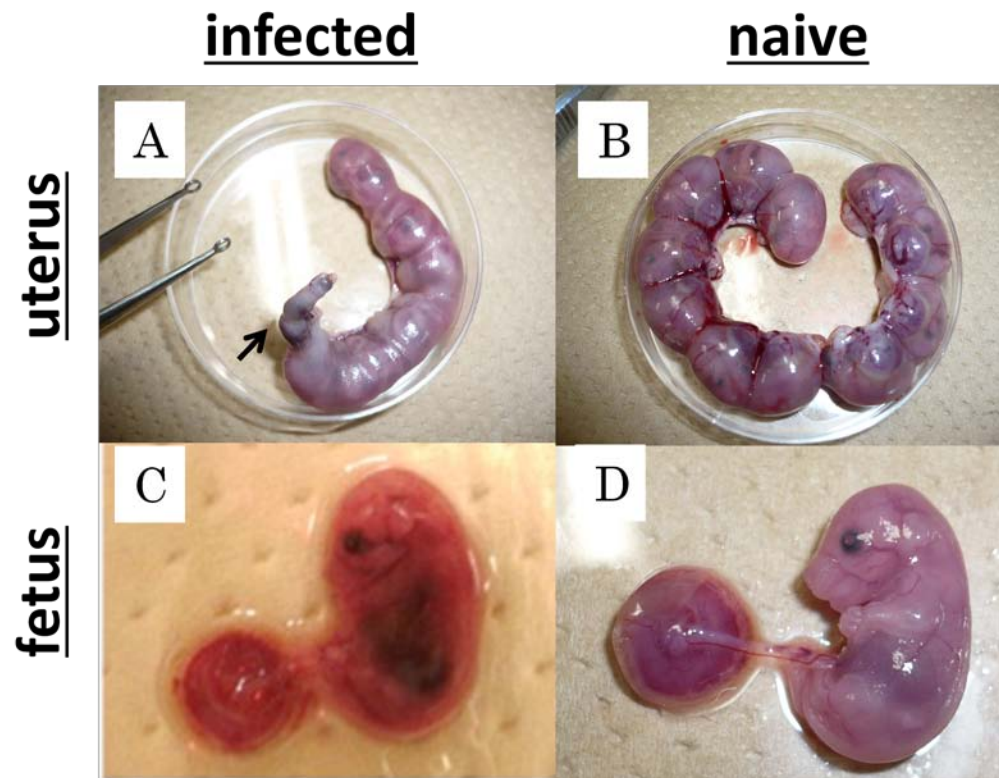


Fig. 27

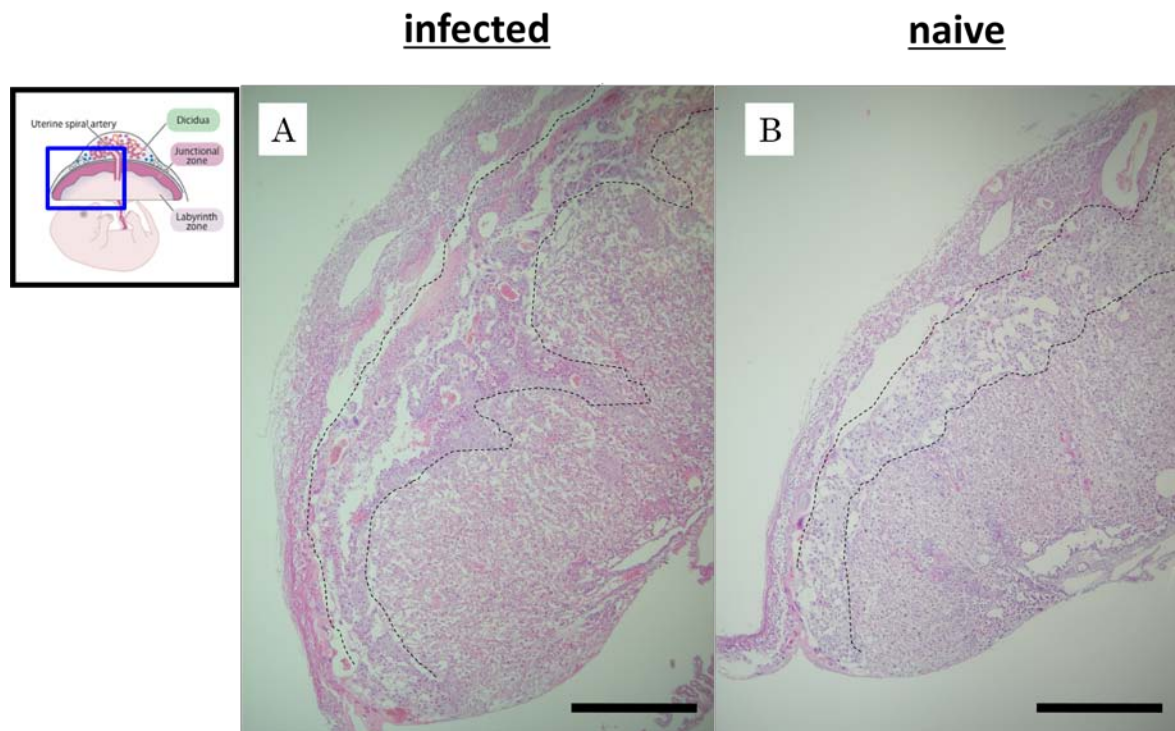


Fig. 28

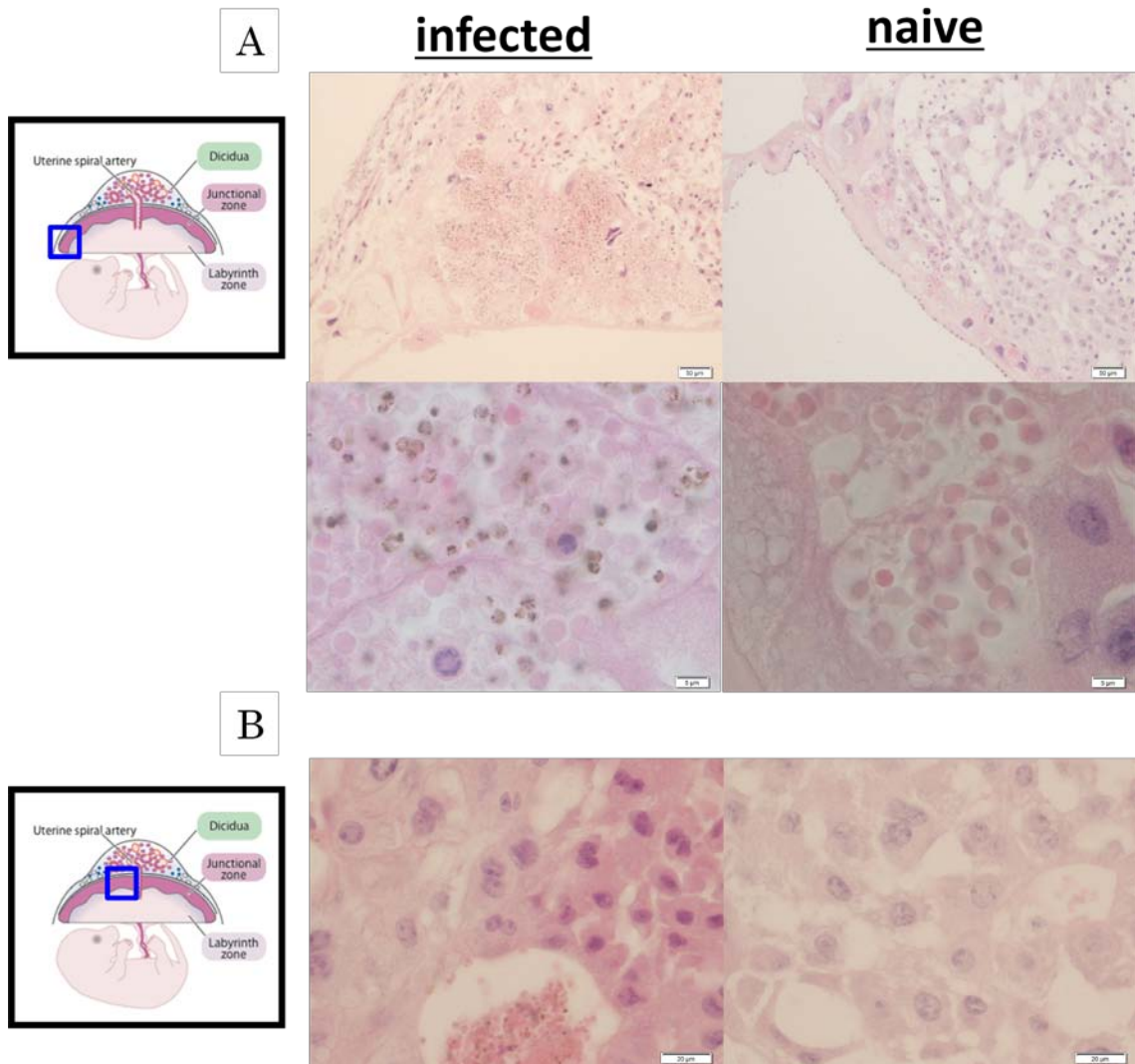


Fig. 29

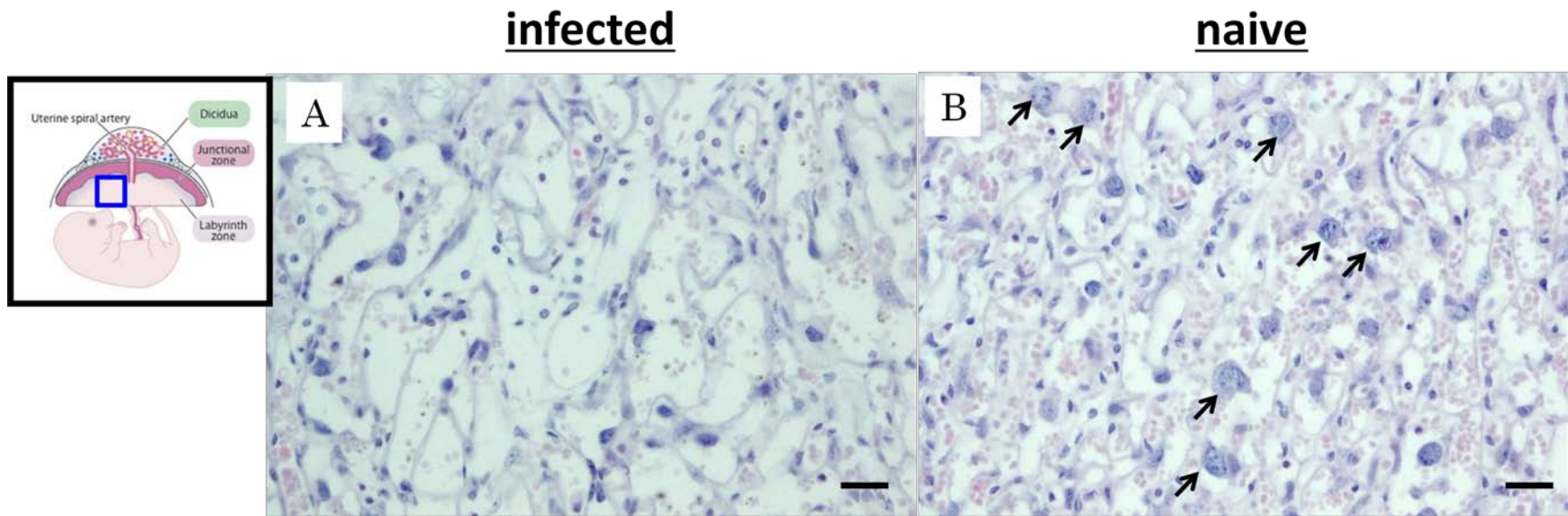


Fig. 30

infected

naive

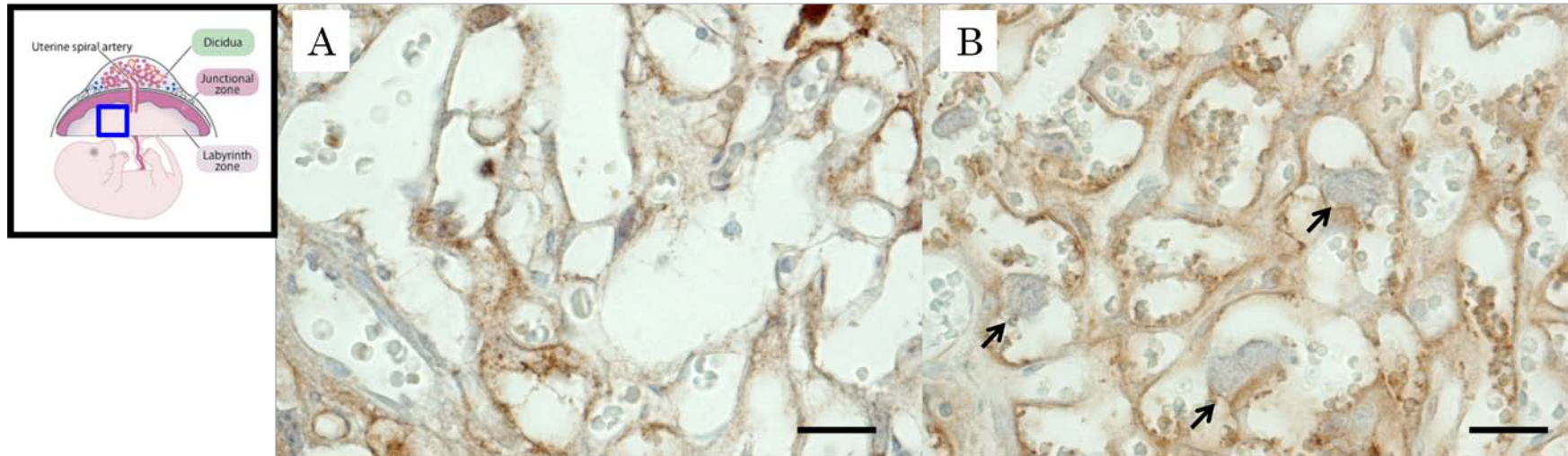
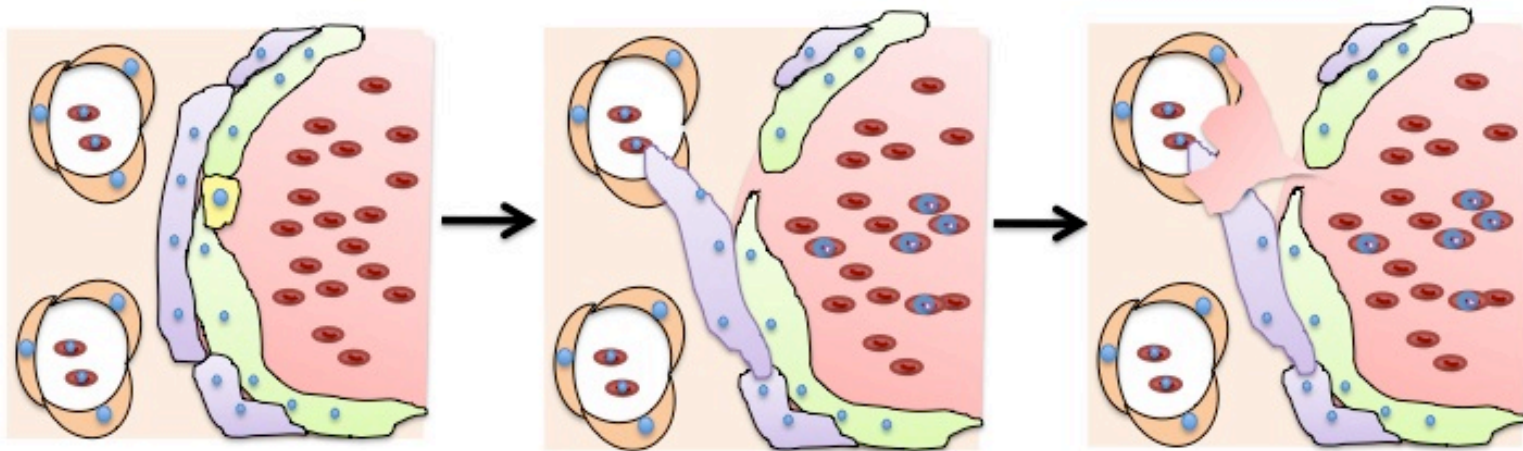


Fig. 31

① maternal *P. berghei* infection

② destruction of placental barrier

③ change the permeability of placental barrier



Stillbirth

poor nutrient supply ?

the failure of the maternal immune tolerance system?

Fig. 32

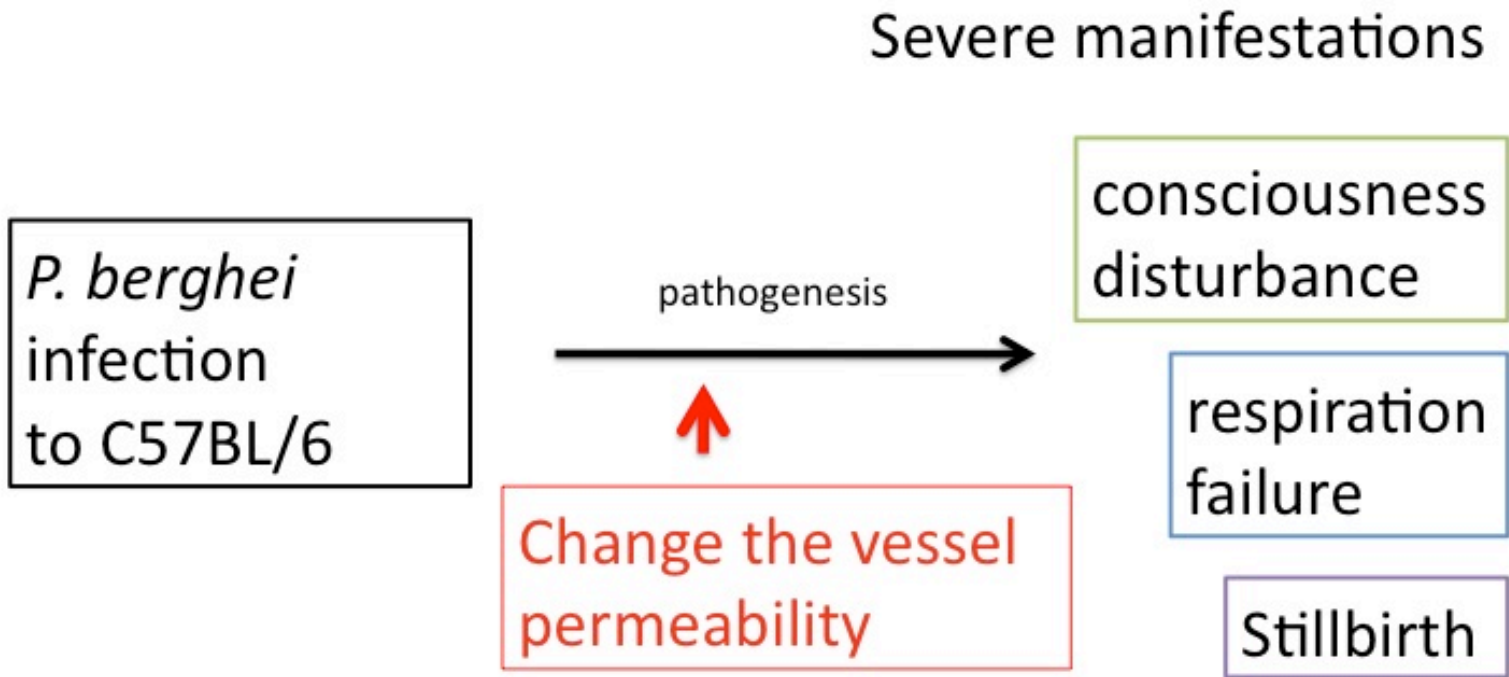


Fig. 33

論文の内容の要旨

応用動物科学 専攻
平成 23 年度博士課程 進学
氏名 山越 祥子
指導教員 松本 芳嗣

論文題目 : Studies on severe manifestations in experimental rodent malaria.

(ネズミマラリアにおける重症症状に関する研究)

Plasmodium 属原虫は寄生原虫のひとつであり、哺乳類の中でもヒトを含む霊長類及び齧歯類、哺乳類以外には爬虫類、鳥類での感染が報告されている。例えばヒトに感染する *Plasmodium* 属原虫は 4 種類あり、ヒトマラリアを発症させる。特に 4 種のうちの 1 つである熱帯熱マラリア原虫(*Plasmodium falciparum*)は原虫血症 (parasitemia) やヒトマラリア三大兆候である発熱、貧血、脾腫に加え脳性マラリア、肺浮腫、腎不全、不正出血を起こす事が知られている。ネズミに感染する *Plasmodium* 属原虫には thicket rat より分離された *P. berghei* を筆頭に *P. chabaudi*、*P. vinckei* 及び *P. yoelli* などが知られている。しかしながら *Plasmodium* 属原虫感染によるマラリアの発症機序は不明な点が多い。本研究では宿主の中でも実験的感染法が確立しているマウスを用いて、ネズミマラリアの病態形成機序の一端を明らかにすることを目的とした。

まず第 1 章ではネズミマラリア原虫 *P. berghei* を実験的に 2 系統の近交系 (C57BL/6、

BALB/c)マウスに感染させ、どのような症状が起きるかを明らかにするため血液検査、行動評価及び剖検を行った。*P. berghei* ANKA 株感染赤血球 1×10^6 個を腹腔内接種することにより C57BL/6 及び BALB/c に致死的な感染をおこさせた。感染 3 日目より両系統共に末梢血中に感染赤血球が認められ、その割合は感染 3 日目より急激に上昇し、感染 6 日目には約 40%となった。ヘマトクリット値は両系統共に感染が進むにつれ著しく減少した。両系統共に感染 5 日目より立毛が認められ、感染 6 日目には踞る姿勢が観察された。C57BL/6 は感染約 7 日目に、BALB/c は感染約 8 日目に死亡した。感染 6 日目に C57BL/6 でのみ顕著な体重減少及び呼吸数の低下が認められた。マウスの運動障害及び意識障害を rapid murine coma and behavior scale (RMCBS)でスコア化した結果、C57BL/6 でスコアが顕著に減少した。感染 6 日目にマウスを安楽殺して剖検した結果、感染マウス脾臓重量は非感染マウスと比較し約 3 倍に達した。さらに C57BL/6 において皮膚での点状赤斑が認められた。以上の結果より *P. berghei* 感染 C57BL/6 及び BALB/c においては原虫血症や脾腫といったマラリア原虫感染に典型的な症状が見られた。また、parasitemia の上昇率は同程度であるにも関わらず C57BL/6 でのみ体重減少、意識障害や運動障害、さらに呼吸不全及び皮膚での異常出血が起きていた。以上第 1 章では *P.berghei* の実験的感染によってマウスに様々な症状が起き、さらに BALB/c に比べ C57BL/6 でより重篤ないくつかの症状がみられる事が明らかになった。

第 2 章、第 3 章では第 1 章において C57BL/6 で認められ、特に顕著な症状であった意識障害、呼吸不全に着目した。これら重症症状の発症機序の一端を血管機能の異常という観点から明らかにする事を目的として解析を行った。

第 2 章では第 1 章で認められた意識障害の発症機序の一端を明らかにするため脳の解析を行った。*P. berghei* ANKA 株感染赤血球 1×10^6 個を C57BL/6 に腹腔内接種した。まず、感染マウスにおいて血液脳関門(Blood-brain barrier; BBB)の破綻を疑い、感染 6 日目にマウス尾静脈より Evans blue 溶液を投与し、1 時間後マウスを安楽殺して心臓より PBS を投与する事により血管内の血液還流を行った。結果、脳実質への高度な Evans blue の浸出が示された。次に感染 6 日目にマウスを安楽殺して脳を採取、HE 染色を行った。結果、大脳皮質領域の毛細血管内では赤血球が減少し、白血球の集中像が観察された。しかしながら血球成分の脳実質への浸出は認められなかった。そこで血漿成分である IgG に対する抗体を用いた免疫組織化学的解析を行った結果、大脳皮質の毛細血管だけではなく、その周囲実質も陽性反応を示した。以上の結果より *P. berghei* 感染末期の C57BL/6 の大脳皮質領域では毛細血管の透過性が亢進し、IgG を含む血漿成分が脳実質へ浸出する事が示唆された。ここから血漿成分の脳実質への浸出が脳浮腫をおこし、意識障害の病態形成の一助を担っていると考えられる。

第 3 章では第 1 章で特に顕著な症状を示した呼吸不全の病態形成機序の一端を明らかにするため肺の解析を行った。*P. berghei* ANKA 株感染赤血球 1×10^6 個を C57BL/6 に腹腔内接種し、感染 6 日目にマウスを安楽殺して肺を採取、HE 染色を行った。非感染マウス肺では毛細血管や II 型肺胞上皮細胞が明瞭に観察されたのに対して、感染マウス肺では毛細血管内に鬱血像が観察され、肺胞壁の肥厚が認められた。さらに、一部の肺胞腔内が薄赤色に染色された事から液体成分が肺胞腔内に貯留していたと考えられる。次に感染マウスでの肺毛細血管の透過性の変化を Evans blue 投与方法により検討した。感染 6 日目にマウス尾静脈より Evans blue 溶液を投与し、1 時間後マウスを安楽殺して心臓より PBS を投与する事により血管内の血液還流を行った。結果、感染マウスの肺全体が濃く青く染色された。ここから毛細血管からの Evans blue の顕著な浸出が示され、肺胞の毛細血管の透過性が顕著に亢進している事が示唆された。以上の結果より *P. berghei* 感染末期の C57BL/6 の肺では毛細血管の透過性が著しく亢進する事で一部の肺胞腔内へ血漿成分が浸出すると考えられる。ここから肺浮腫がおき、呼吸不全発症の一助を担っていると考えられる。以上、第 2 章、第 3 章では C57BL/6 で認められた意識障害及び呼吸不全の発症機序に血管透過性の変化が関与する事が明らかになった。

第 4 章では妊娠期に特異的に形成され、胎仔の発育に重要な役割を担う血管集合体である胎盤に着目して *P. berghei* が母体に感染した際の胎盤の病理学的変化を詳細に解析した。まず、*P. berghei* が母体に感染する事が胎仔に与える影響について検討した。C57BL/6 を交配し、交配翌日に膣栓を確認した日を gestation day 1(G1)とした。G13 に *P. berghei* ANKA 株感染赤血球 1×10^7 、 10^6 及び 10^5 個をそれぞれ腹腔内接種して出産時の仔の死亡率及び重量を検討した。結果、仔の死亡率は非感染では 15%であったのに対して、順に 100%、64.71%、21.05%であった。また仔の重量は非感染では 1.26 g であったのに対して順に 0.76 g、0.98 g、1.18 g であった。よって母体が *P. berghei* 感染する事で胎仔の生存率の低下及び重量の減少を起し、死産や低体重症を起す事が分かった。次に新生仔の死亡率が顕著であった 1×10^7 感染母体での胎盤の病理学的変化を検討した。G13 に *P. berghei* ANKA 株感染赤血球を 1×10^7 個を腹腔内接種し、G18 に母体を安楽殺して胎仔の生存数を検討すると共に胎盤を採取し HE 染色を行った。結果胎仔は全て死亡していた。マウスの胎盤は母体側より decidua、junctional zone 及び labyrinth zone の 3 層の細胞層より構成されているが感染母体の胎盤では junctional zone が labyrinth zone に異常に貫入し、また junctional zone に赤血球の集中像が認められた。Labyrinth zone では大型の核を持つ cytotrophoblast cell 及び syncytiotrophoblast cell が母体血液と胎仔血液を隔てる胎盤関門を構成しているが、感染母体胎盤では cytotrophoblast cell の数が減少した。さらに syncytiotrophoblast cell に特異的に発現する syncytin に対する抗体を用いて免疫組織化学的解析を行った結果、感染母体胎盤では染色部位の減少が認められた。ここか

ら syncytiotrophoblast cell が破壊され、maternal blood space の拡張が示唆された。以上の結果より 1×10^7 *P. berghei* 感染母体では出産前に母体胎内で胎仔が死亡し、この時胎盤構造の著しい変化が起きている事が初めて明らかになった。特に胎盤関門を構成している cytotrophoblast cell 及び syncytiotrophoblast cell の消失及び破壊は母体マウスの血流の異常を起し、胎仔の症状に深く関わりと考えられる。

本研究により、ネズミマラリア原虫感染によっておこるいくつかの重症症状が明らかとなり、さらに血管透過性の変化がこれらの病態形成の一助を担っている事が示唆された。本研究によりネズミマラリアにおける重症症状の病態形成機序の一端が明らかとなり、これらの病態形成機序論に新たな一説を提供すると共に *Plasmodium* 属原虫感染によって起こるマラリアの発症機序解明に大きく貢献すると考えられる。